Q. J. R. Meteorol. Soc. (2005), **131**, pp. 639–673 doi: 10.1256/qj.04.13

Microstructures and precipitation development in cumulus and small cumulonimbus clouds over the warm pool of the tropical Pacific Ocean

By ARTHUR L. RANGNO and PETER V. HOBBS*
Department of Atmospheric Sciences, University of Washington, Seattle, USA

(Received 3 February 2004; revised 23 August 2004)

SUMMARY

In situ airborne measurements obtained in convective clouds in the vicinity of the Marshall Islands on 15 days in July and August 1999 are used to determine the microphysical structures and precipitation-producing mechanisms in these clouds. The liquid water contents of the clouds were generally well below adiabatic values, even in newly risen turrets. This is attributed to the entrainment of ambient air and to the very efficient removal of cloud water by the collision and coalescence of drops. The formation of raindrops began when the concentration of droplets with radii >15 μm exceeded $\sim$3 cm^{-3} or, equivalently, when the effective cloud drop radius reached $\sim$13 μm. Clouds rained when their depth exceeded $\sim$1.5 km. Due to rainout, the effective radius of cloud droplets began decreasing $\sim$2–4 km above cloud base.

Extremely high concentrations of ice particles (often $>$500 litre^{-1}) formed very rapidly at temperatures between -4 and -10 °C. High-resolution imagery of these particles, which were primarily sheaths, needles, frozen drops and irregular ice fragments, indicates that the high concentrations of ice were initiated by the freezing of individual drops, some of which fragmented upon freezing, accompanied by ice splinter production during riming. However, for ice particles <100 μm in maximum dimension, frozen drops and ice fragments were much more numerous than columnar ice crystals, the latter being indicative of ice splinter production. Narrow (10–50 m wide) streamers of precipitation containing large ($>$3 mm diameter) solid and liquid particles were often encountered in growing clouds. It is proposed that the particles in these streamers grew rapidly by riming in water-rich zones and, under appropriate conditions, the ice particles produced by both drop fragmentation and riming resulted in exceptionally high localized concentrations of ice. Convective clouds consisting entirely of liquid water produced rain rates that were similar to those from deep convective clouds containing ice.

Since the concentration of drizzle and raindrops within a few kilometres of cloud base was highly correlated with cloud depth, and therefore cloud top temperature, the concentration of raindrops in cumulus and cumulonimbus clouds over the warm pool of the tropical Pacific Ocean can be inferred from satellite measurements of cloud top temperatures.

KEYWORDS: Cloud structures Convective clouds Pacific warm pool Precipitation mechanisms

1. INTRODUCTION

In previous papers we reported on cloud microstructures and precipitation development in polar marine cumuliform clouds (Hobbs and Rangno 1985, 1990; Rangno and Hobbs 1991), mainly polar continental cumuliform clouds (Rangno and Hobbs 1994), and arctic stratiform clouds (Hobbs and Rangno 1998). In this paper we describe the microstructures and development of precipitation in cumuliform clouds over the tropical Pacific warm pool.

Over the past few decades interest in convective clouds over the tropical oceans has increased with the realization of the roles they play in the heat budget of the atmosphere and in teleconnections with middle latitudes (e.g. Bjerknes 1969; Hou 1998). Also, the Tropical Rainfall Measuring Mission (TRMM) satellite has provided the potential for measuring rainfall from tropical clouds, provided certain assumptions are made concerning the size distribution of precipitation particles and their radar backscatter characteristics (Simpson *et al.* 1986, 1988; Kingsmill *et al.* 2004). Therefore, to augment previous studies of these topics (e.g. Malkus 1954; Malkus and Ronne 1954; Ackerman 1959; Leary and Houze 1979; Gamache 1990; Yuter and Houze 1998), it is an appropriate time to report on recent measurements of the microstructures of tropical clouds and the processes by which they produce precipitation.

* Corresponding author: Department of Atmospheric Sciences, University of Washington, Box 351640, Seattle, Washington, 98195-1640, USA. e-mail: phobbs@atmos.washington.edu

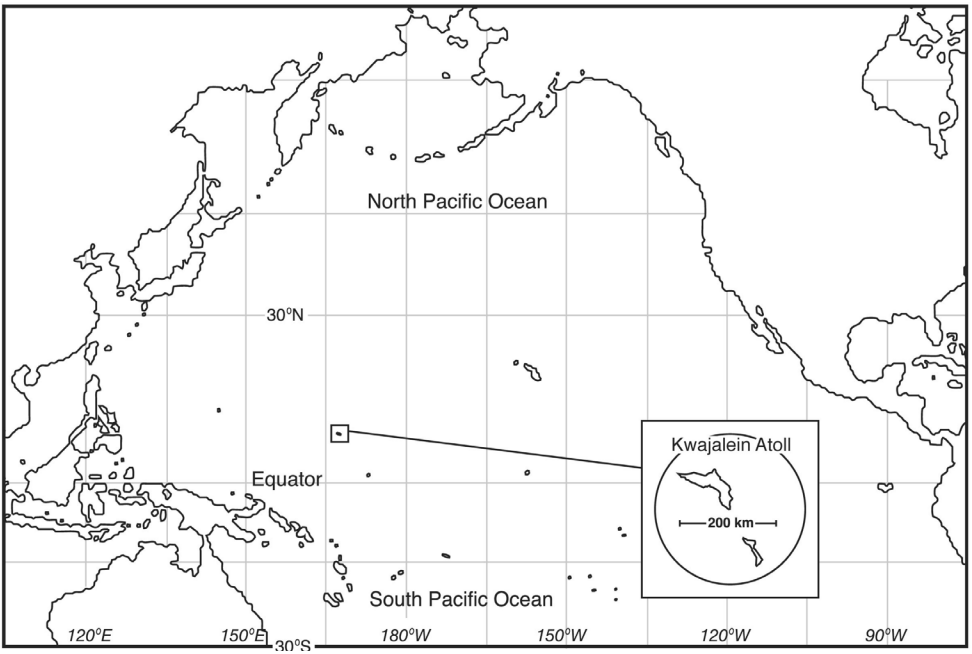

Figure 1. Location of the Kwajalein Atoll, Marshall Islands, in the western Pacific Ocean. The inset shows the research area covered by the University of Washington's Convair-580 aircraft from 25 July to 30 August 1999 in the Tropical Rainfall Measuring Mission (TRMM)/Kwajalein Experiment (KWAJEX) field study.

This paper is based on *in situ* measurements obtained aboard the University of Washington's (UW) Convair-580 research aircraft in the TRMM/Kwajalein Experiment (KWAJEX), which was carried out in the intertropical convergence zone in the vicinity of the Kwajalein Atoll, Republic of the Marshall Islands (Fig. 1), from 25 July to 30 August 1999. Measurements obtained in KWAJEX aboard a higher-flying aircraft have been described by Stith *et al.* (2002, 2004), selected microphysical datasets from KWAJEX have been documented by Kingsmill *et al.* (2004) primarily for the purpose of comparisons with TRMM satellite measurements, and Yuter *et al.* (2005) have described some characteristics of the convection observed in KWAJEX.

In this paper we address the following questions for the small to moderate sized convective clouds (tops <9 km above mean sea level (amsl)) sampled aboard the UW aircraft in KWAJEX. What were the droplet-size spectra and droplet concentrations? What were the vertical profiles of cloud liquid water content (CLWC)? Under what conditions did the collision–coalescence process for the formation of raindrops begin? Did giant particles play a role in the formation of large drops? At what cloud depths did rain form? At what temperatures did ice particles begin to appear? What processes were responsible for the formation of ice? What role did ice play in the formation of precipitation? How do the results from this study compare with those for clouds in other regions?

2. Instrumentation

CLWC was measured with a Droplet Measurement Technologies (DMT) hot-wire device, which measures the CLWC of droplets in the diameter range 10–40 μm. The CLWC of droplets from ~2–47 μm in diameter could also be derived from measurements of the size spectrum of droplets with a Particle Measuring Systems (PMS) Forward Scattering Spectrometer Probe (FSSP)-100. The FSSP-100 was calibrated three

times during KWAJEX, using glass beads of known sizes and a DMT micro-positioner calibration device. The liquid water contributed by larger cloud drops and drizzle drops (50–500 μm diameter) was derived from drop spectrum measurements made using a PMS 2D-cloud probe (2D-C). Cloud particle-size distributions and concentrations over the diameter range 25–1 mm were measured with the 2D-C, and the size distribution of precipitation particles from 100 μm to about 9 mm diameter was measured with a PMS 2D precipitation probe (2D-P), using particle reconstruction software to estimate the sizes of particles that extend beyond the width of the diode arrays of these probes (Heymsfield and Parrish 1978).

Two new particle imaging probes were aboard the UW aircraft: a Stratton Park Engineering Company (SPEC) high-volume precipitation sampler (HVPS), and a SPEC cloud particle imager (CPI). These probes have been described by Lawson *et al.* (1993) and Lawson and Jensen (1998), respectively. The HVPS provides better statistical measurements of the largest precipitation-sized particles than the 2D-P, because it has a sampling volume of $\sim$1 m^{3}s^{-1} at an aircraft speed of 100 m s^{-1} compared to $\sim$0.07 m^{3}s^{-1} for the 2D-P. The HVPS has a fixed resolution (pixel size) of 200 μm, and can image particles up to $\sim$6 cm in maximum dimensions. The splashing of drops and the breakup of aggregated ice particles on the leading edge of the HVPS (or perhaps due to their acceleration in the vicinity of the probe) resulted in artifacts that were sometimes difficult to remove. However, the HVPS particle-size spectra were generally in good agreement over time periods of $\sim$10 s to 1 minute with those derived from the 2D-P.

The most important probe for the classification of ice particles, and for differentiating small ice particles from droplets, was the CPI. The CPI can be used to distinguish small non-spherical ice particles from water droplets for particles down to $\sim$20–40 μm in maximum dimensions. For comparison, phase discrimination in the 2D-C imagery is limited to particles no smaller than $\sim$100–150 μm in maximum dimensions. The imagery from the CPI was processed using software provided by SPEC for the sizing of particles. However, the phase and type of particle were determined manually. Due to some uncertainty in the concentrations of particles measured by the CPI (SPEC 2000), these concentrations are not used in this paper.

Atop the fuselage of the UW Convair-580 a clear plastic hemispherical dome provides a 360° view. This was invaluable for the characterization of features of cloud systems, and for the detection of very low concentrations of very large particles that produced audible impacts. At typical aircraft speeds of 90–120 m s^{-1} the dome provided, in effect, a sampling volume in the forward direction of $\sim$3 m^{3}s^{-1}, compared to $\sim$1 m^{3}s^{-1} for the HVPS. Very often the large particles that hit the dome came in audible bursts (like handfuls of rice being thrown at the dome) with durations from one to a few tenths of a second, indicating vertical strands of heavy precipitation only about 10–50 m in width (see Hobbs and Rangno 1985; Rangno and Hobbs 1991).

The aerosol instrumentation aboard the UW Convair-580 in KWAJEX is described by Kaneyasu *et al.* (2001). These instruments provided aerosol-size spectra from $\sim$0.1–47 μm diameter. A condensation nucleus counter for total aerosol concentrations, and a three-wavelength nephelometer for light-scattering measurements, were also aboard. Also, we examined the CPI and the 2D-C imagery in the pursuit of giant or ultra-giant aerosol (>50 μm diameter) particles in the sub-cloud base layer.

3. Definition of a cloud, types of clouds sampled, and flight patterns

We define a cloud as follows. A concentration of at least 10 cm^{-3} of particles measured by the FSSP-100 is used to define a droplet cloud. For clouds consisting entirely of

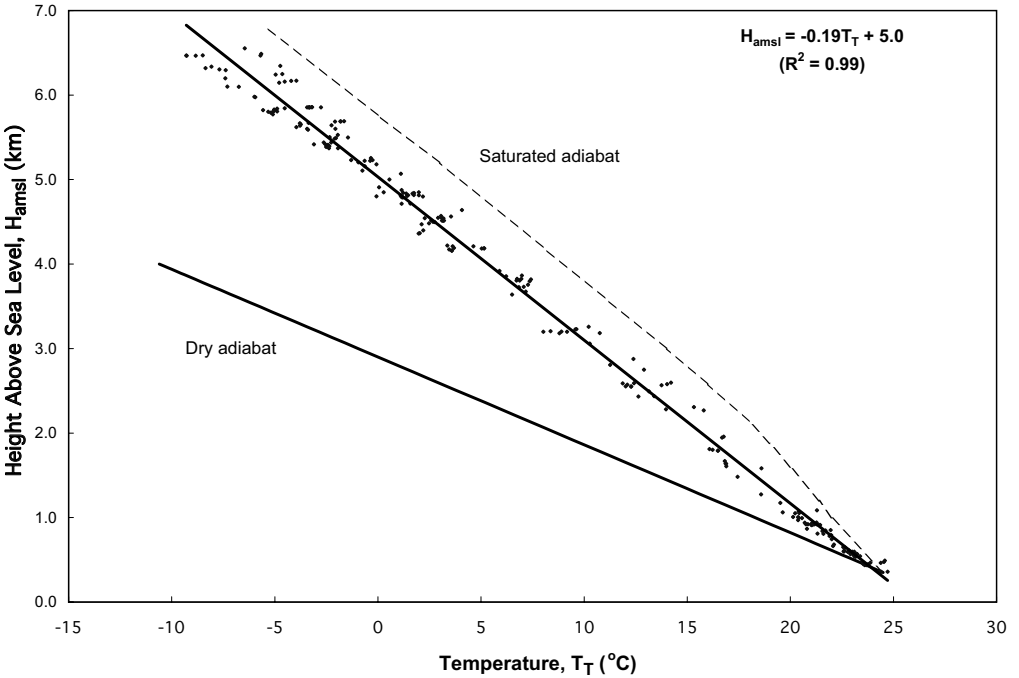

Figure 2. Temperatures in cumuliform clouds versus height above mean sea level in KWAJEX. The least-squares best fit is also shown.

ice, a 2D-C concentration $\geqslant$1 litre^{-1} for particles of maximum dimension >100 μm is defined as a cloud, although many more smaller ice particles were undoubtedly present. The criterion for the presence of a mixed-phase (i.e. water plus ice) cloud is that the FSSP–100 count is >10 cm^{-3} and that measurable concentrations of ice particles are detected by the 2D-C and/or the CPI probe.

The cumuliform clouds sampled from the Convair-580 ranged from cumulus fractus at the top of the sub-cloud layer to large cumulonimbus (some of which produced lightning). Funnel clouds (i.e. partially developed waterspouts that produced disturbances on the water) were seen beneath several cumulus congestus clouds. Middle-level stratiform clouds (altocumulus and the lower portions of altostratus), associated with deep, precipitating shields of anvil ice clouds ejected from cumulonimbus complexes, were also sampled. However, the structures of stratiform clouds, and convective clouds into which rain fell from stratiform regions, are not described in this paper.

Here we focus on measurements obtained on 15 days, from ~756 convective clouds and their immediate glaciated debris. We examine in more detail a subset of ~185 small to moderate sized convective clouds for which either cloud top heights were measured directly or could be accurately derived from the forward video, and which thus provide measurements of cloud depth. These latter clouds were generally considerably smaller in both horizontal and vertical extent than the main cloud complexes seen in satellite imagery in the vicinity of KWAJEX. All of the tops in the small to moderate sized convective clouds were below 10 km amsl, and therefore no colder than about −33 °C. The median cloud top temperature for clouds sampled above the 0 °C level was −5 °C.

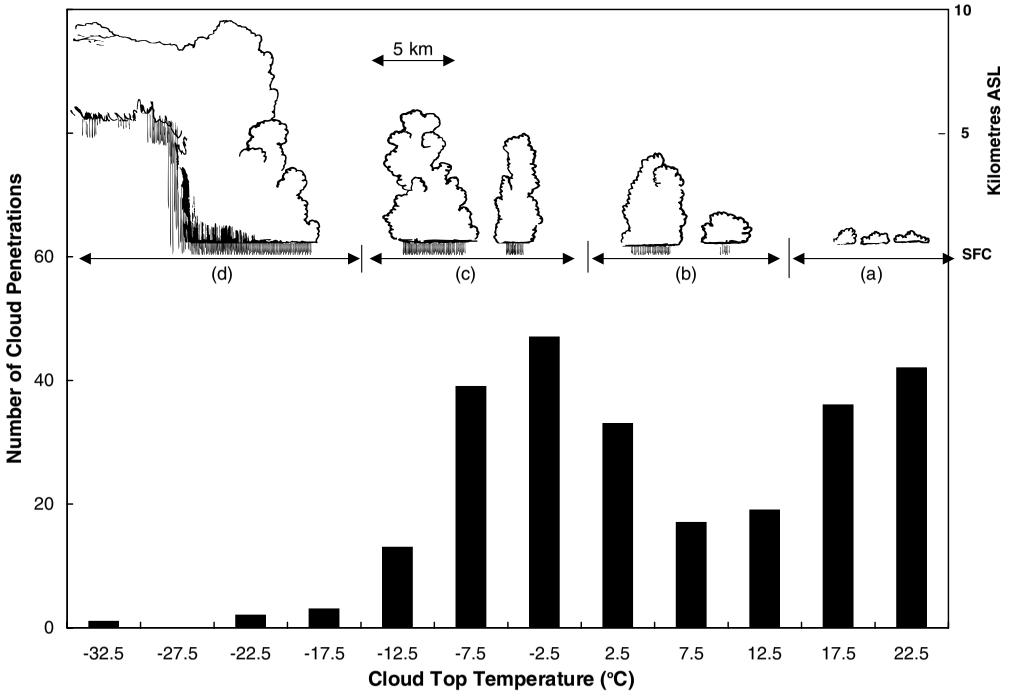

Figure 3. Numbers of penetrations of the various cloud types by the Convair-580 aircraft in KWAJEX for the subset of data where cloud top temperatures were known, with appropriate schematic cloud forms. From the right-hand side: (a) cumulus humilis and cumulus fractus clouds <1.0 km deep (right-hand scale), these were the most numerous of the cumuliform clouds and never produced rain; (b) cumulus congestus and small cumulonimbus calvus clouds 1.5–4 km deep, the shallowest of these produced brief light rain showers, the deepest produced brief heavy rain showers; they contained no subfreezing regions; (c) short-lived, erect and narrow cumulonimbus calvus and cumulus capillatus clouds 4–7 km deep in low wind-shear environments with well-developed shafts of rain; (d) moderate-sized cumulonimbus capillatus clouds >7 km deep with extensive anvil regions and strong shearing of tops above 500 hPa.

Since the temperature in the clouds was a linear function of altitude (Fig. 2), and cloud base height was fairly constant (0.5–0.6 km), cloud depth could be reliably estimated from cloud top temperatures. Figure 3 summarizes the sizes of clouds sampled, as a function of cloud top temperature, for the subset of 185 small to moderate sized convective clouds, and Fig. 4 shows photographs of these clouds. The measurements in isolated clouds were particularly useful, since these clouds often formed the building blocks for cloud clusters. The regional homogeneity of the clouds aided in developing a picture of their structures and the ways in which precipitation developed within them.

Horizontal legs were also flown just above and just below the melting level in mesoscale convective cloud clusters (hereafter referred to simply as 'cloud clusters'). These provided considerable data on the concentrations of ice particles and raindrops in the major rain-producing systems of the region. Some of the cloud clusters were sampled more than once at nearly the same altitude, which provided information on their evolution at these levels.

At temperatures below −5 °C aircraft can produce ice particles when flying in clouds (Rangno and Hobbs 1983). However, in KWAJEX the Convair-580 flew mainly in the lower portions of clouds up to the freezing level; periods in which it flew at temperatures below −5 °C were relatively few. Post-examination of the imagery and flight tracks suggests that on just one occasion, for a duration of 3 s, the Convair-580

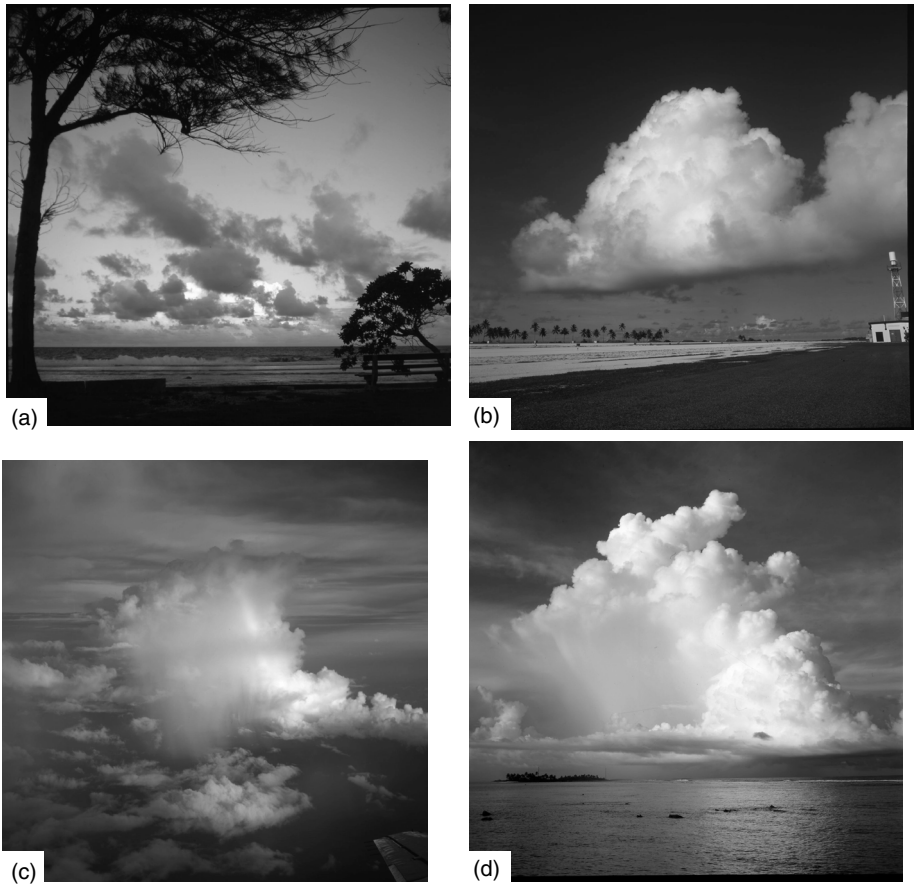

Figure 4. Photographs of the types of more isolated clouds from which cloud top temperatures, heights, and thus cloud depths, were deduced, and on which this study is focused: (a) cumulus fractus and cumulus humilis; (b) cumulus mediocris of the size typical of those from which the first raindrops fell (a very slight vertical shading due to a transparent rain shaft can be seen below the tallest peak of the cloud from the cloud base downwards); (c) small isolated cumulonimbus capillatus cloud formed completely below the freezing level; the cloud is raining out, and is illustrative of the high efficiency of the coalescence process in the Pacific warm pool (note the faint rainbow that extends from the top of the cloud down its side); (d) moderate sized isolated cumulonimbus capillatus cloud, the tops of which extended well above the freezing level.

intercepted ice particles that might have been produced by a previous pass through the cloud at −9 °C. These 3 s of data were excluded from the present study.

4. Results

(*a*) *Overview of cloud properties*

Figure 5 shows the number of droplet clouds (either liquid or supercooled) of various widths in which our measurements were obtained. The fact that the results fall roughly on a straight line on the log probability plot shown in Fig. 5, implies that the widths of the clouds sampled were nearly log-normally distributed.

Table 1 summarizes some of the principal properties of the convective clouds sampled over the Pacific warm pool near Kwajalein, Marshall Islands. Cloud base temperatures averaged 24.5 °C; the ranges of cloud base temperatures (22–26 °C) and

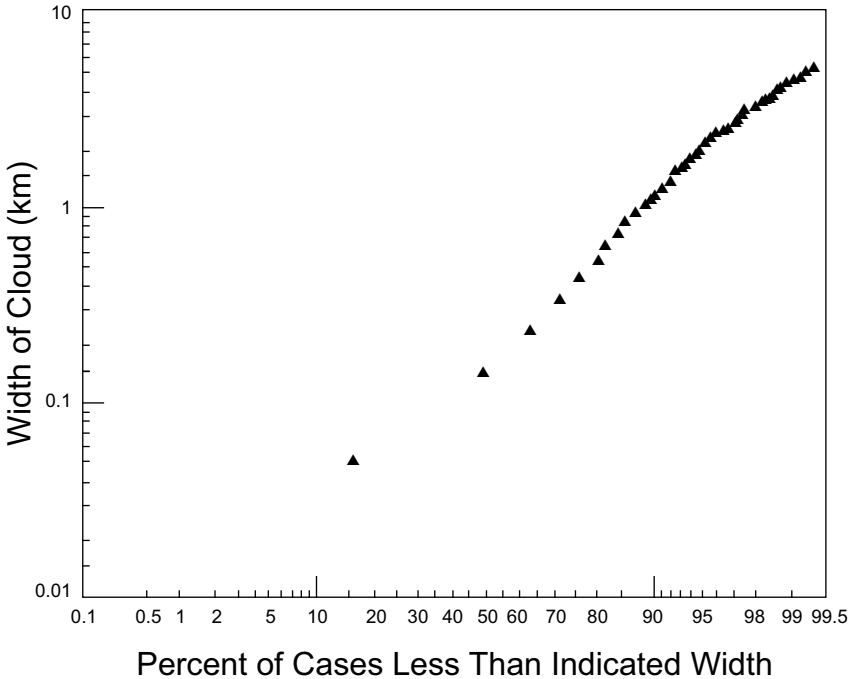

Figure 5. Log probability plot for the widths of clouds sampled from the Convair-580 aircraft in KWAJEX.

heights (290–610 m amsl) encountered were relatively small. Lower cloud bases than these, in the form of arcus or shelf clouds, were observed in the outflow air from large mature cumulonimbus complexes. At the average cloud base pressure and temperature of 963 hPa and 24.5 °C, respectively, the water vapour mixing ratio was 20 g kg^{-1}. Average cloud droplet concentrations ($\sim$70 cm^{-3}) were typical of marine clouds and generally varied little from day-to-day (Table 1), although peak concentrations, presumably in updraughts, exceeded 300 cm^{-3} (Table 1).

If the turrets of single, newly risen cumulus clouds briefly reached the -5 °C level, or even somewhat lower temperatures, before falling back to lower heights and higher temperatures, they continued to be composed of water droplets, drizzle and raindrops. However, turrets that reached heights where the temperature was -10 °C or lower, or turrets that resided for more than a few minutes between the -5 and -10 °C levels, developed appreciable concentrations of ice.

Extraordinarily high concentrations of ice particles (often $>$500 litre^{-1}) with maximum dimensions $>$100 μm were frequently encountered between the freezing level and -10 °C in fully developed cumulonimbus clouds with tops far above the -10 °C level. Most of these particles appeared to be needles and sheaths. Sometimes the ice particles consisted of columnar ice elements with lengths $<$400 μm, together with substantial supercooled water and either none or just a few small ice aggregates. Since needles and sheaths grow at about 1 μm s^{-1} where the air is saturated with respect to water at -7 °C (Pruppacher and Klett 1997), this indicates that the high concentrations of columnar ice particles had grown to these sizes within a few minutes.

Ice particles with maximum dimension $<$100 μm (which were not included in the high concentrations mentioned above) presented a different picture; these were mainly frozen drops and ice fragments.

TABLE 1. SUMMARY OF PROPERTIES OF CUMULIFORM CLOUDS SAMPLED BY CONVAIR-580 NEAR KWAJALEIN, MARSHALL ISLANDS, JULY/AUGUST 1999

Date	A	B	C	D	E	F	G	H	I	J	K	L	M	N
25 July	1783	27	977	0.30	24.5	105	90	270	5.02	−2.0	0.90	0.79	0.75	1.15
28 July	1784	116	965	0.43	24.0	90	90	190	6.47	−8.6	1.95	1.67	2.58	0.76
30 July	1785	33	974	0.35	24.0	45	37	130	6.45	−7.6	3.05	2.41	4.13	0.74
1 Aug	1786	6	940	0.60	22.0	85	75	–	3.22	9.2	3.29	3.20	5.82	0.57
3 Aug	1788	9	980	0.29	24.5	60	45	–	3.21	8.0	3.11	2.88	5.16	0.60
6 Aug	1789	39	955	0.47	24.0	90	80	310	4.88	−1.0	3.31	1.40	3.63	0.91
9 Aug	1791	150	959	0.45	24.5	75	60	370	6.51	−9.8	2.32	4.46	4.77	0.49
11 Aug	1792	3	970	0.38	23.5	75	75	–	2.54	10.8	2.64	2.59	4.52	0.58
23 Aug	1793	7	960	0.50[1]	24.0[1]	80	85	–	4.97	−1.8	0.92	NA	9.39	0.10
24 Aug	1794	97	961	0.47	24.0	65	65	180	5.86	−6.2	2.08	1.59	2.51	0.83
25 Aug	1795	66	939	0.61	23.0	55	35	280	5.90	−6.2	1.72	4.88	7.34	0.23
26 Aug	1796	85	969	0.36	26.5	65	60	240	5.94	−3.0	2.49	1.43	2.17	1.15
27 Aug	1797	34	957	0.45	25.0	60	60	200	5.86	−4.1	1.70	4.17	9.49	0.18
28 Aug	1798	39	961	0.42	25.5	50	35	210	6.24	−5.7	1.58	4.07	5.78	0.27
30 Aug	1799	45	981	0.29	26.5	35	25	120	6.55	−8.5	2.09	3.66	6.83	0.31
	Total	756												
	Average		963	0.419	24.4	69	61	227	5.31	−2.4	2.21	2.80	4.99	0.59
	Median		963	0.424	24.3	65	60	210	5.86	−4.1	2.09	2.74	4.77	0.58
	Standard deviation		13.1	0.1	1.2	19	22	76	1.33	6.7	0.78	1.31	2.54	0.33
	Maximum		981	0.608	26.5	105	90	370	6.55	10.8	3.31	4.89	9.49	1.15
	Minimum		939	0.285	22.0	35	25	120	2.54	−9.8	0.90	0.79	0.75	0.10

[1]Estimated values.
A. University of Washington flight number.
B. Number of cumuliform clouds sampled.
C. Cloud base pressure (hPa).
D. Cloud base height (km, amsl).
E. Cloud base temperature (°C).
F. Average droplet concentration (cm^{-3}).
G. Median droplet concentration (cm^{-3}).
H. Average of ten highest 1 s droplet concentrations (cm^{-3}).
I. Highest altitude at which a cloud was sampled (km).
J. Lowest temperature measured in cloud (°C).
K. Maximum cloud liquid water content (CLWC) ($g\ m^{-3}$).
L. Altitude where maximum CLWC was measured (km).
M. Adiabatic CLWC at the level where maximum CLWC was measured ($g\ m^{-3}$).
N. 'Adiabaticity', defined as the ratio of the measured CLWC to the adiabatic CLWC at the level where the maximum CLWC was measured.

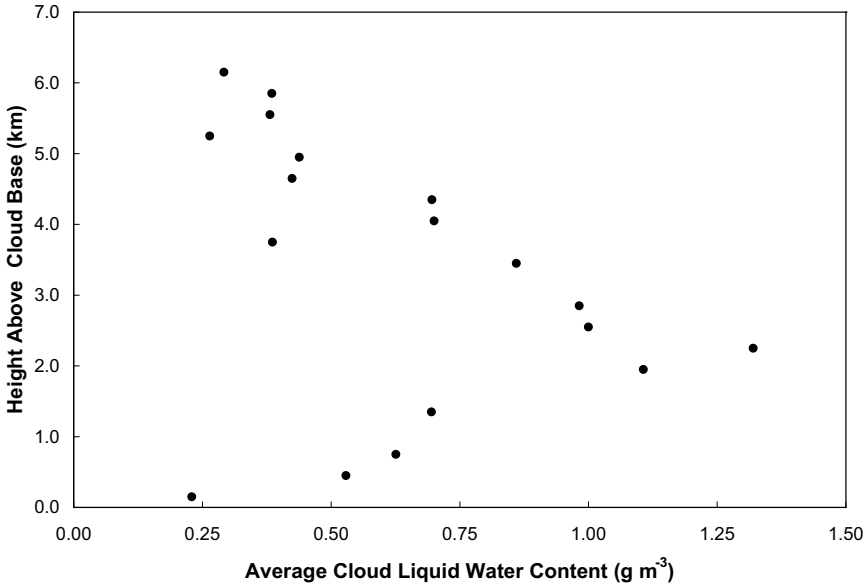

Figure 6. Average cloud liquid water content versus height above cloud base in cumuliform clouds with droplet concentrations of $\geqslant 100$ cm^{-3} measured from the Convair-580 aircraft in KWAJEX.

(*b*) *Profiles of liquid water and the growth of cloud drops by collision–coalescence*

Figure 6 shows the average CLWC measured at various heights above cloud base for all of the cumuliform clouds sampled. The maximum in the average CLWC occurred at ~2 km above cloud base, or at a pressure level of only ~800 hPa.

Following Hobbs and Rangno (1985), the broadness of the droplet-size distribution can be represented by the 'droplet threshold diameter', D_T, which is defined as the droplet diameter for which the total concentration of droplets with greater diameter is 3 cm^{-3} (as measured by the FSSP-100). Figure 7 shows D_T as a function of height above cloud base. It can be seen from this figure that clouds with depths $\geqslant 1$ km begin to contain appreciable concentrations of drops >30 μm in diameter. Such drops have the potential to collect smaller droplets and to grow by the collision–coalescence process into raindrops. Drizzle drops and raindrops were, in fact, observed beneath all clouds with depths exceeding ~1.5 km. Also shown in Fig. 7, for comparison, are measurements in marine cumuliform clouds over the Azores (cloud base temperature ~18 °C) and over the coastal waters of Washington State (cloud base temperature ~3 °C). The measurements in the Azores closely resemble those obtained in KWAJEX; however, for the Washington State coastal clouds slightly smaller values of D_T were associated with the onset of drizzle and (small) raindrops than for either the Azores or Marshall Island clouds.

Another measure of the overall broadness of the droplet-size distribution is the effective radius (r_e) of the droplets, defined as:

$$r_e = \int_0^\infty r^3 n(r)\,\mathrm{d}r \Big/ \int_0^\infty r^2 n(r)\,\mathrm{d}r,$$

where $n(r)$ is the number concentration of droplets with radii between r and $r + \mathrm{d}r$. The variation of r_e with height above cloud base (Fig. 8) is somewhat similar to that of D_T, in that r_e initially increases with height but subsequently decreases slightly

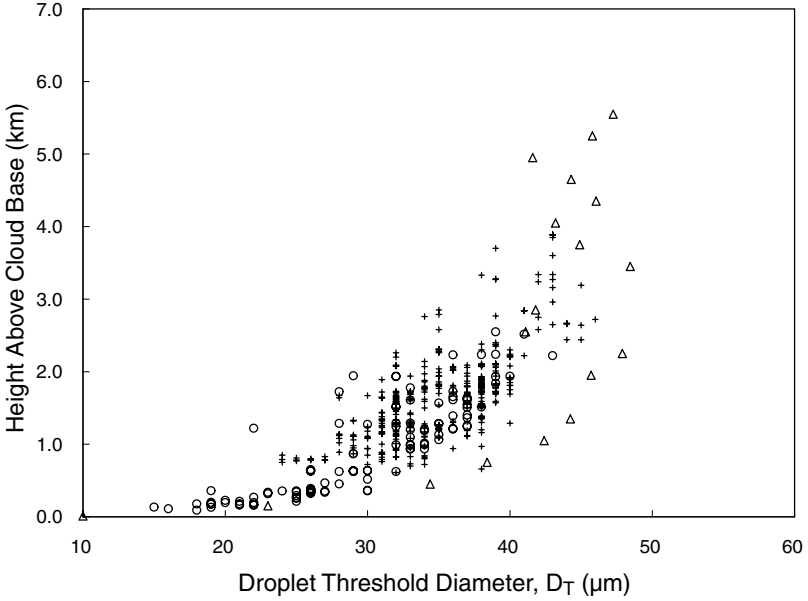

Figure 7. Average of the maximum droplet threshold diameters (D_T) versus height above cloud base for cumuliform clouds sampled from the University of Washington aircraft: in KWAJEX (triangles); in marine cumuliform clouds over the Azores (crosses); and over coastal waters off Washington State (circles). See text for details.

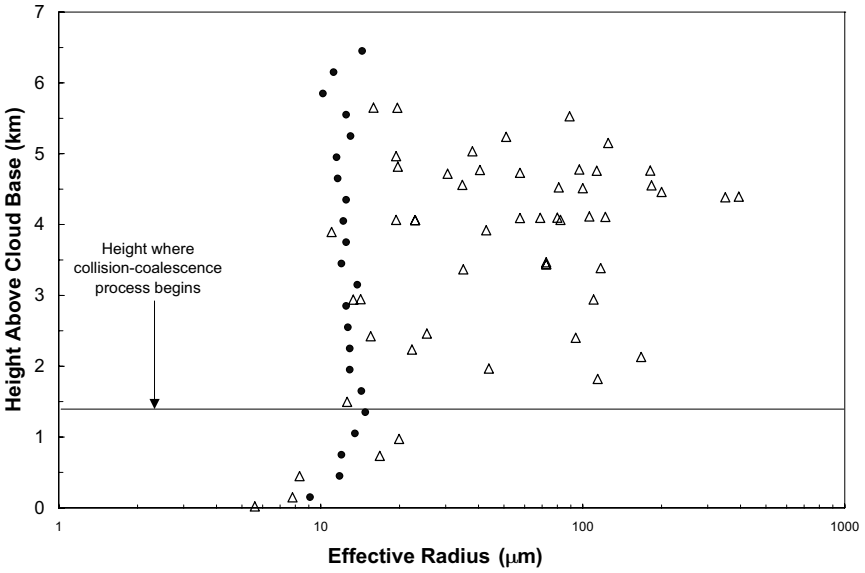

Figure 8. Average of the maximum effective droplet radii (r_e) versus height above cloud base for cumuliform clouds sampled from the University of Washington Convair-580 aircraft in KWAJEX. Solid circles denote r_e calculated from the FSSP-100 for droplets <50 μm diameter; triangles denote r_e calculated from the FSSP-100 and the 2D-C for drops from ~ 50 μm to about 1 mm diameter. See text for details.

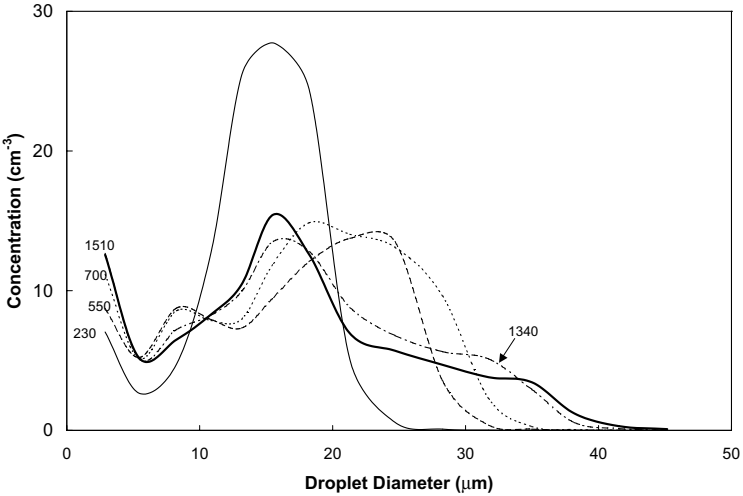

Figure 9. Examples of droplet-size spectra averaged over height intervals of ~300 m for cumulus fractus to small cumulus congestus clouds sampled on 24 August 1999 from the Convair-580 aircraft in KWAJEX. The curves are labelled with the average heights (m) of the measurements. The maximum average height of 1510 m above cloud base is very near the tops of the clouds.

when only cloud-sized droplets (<50 μm diameter) are considered (solid circles in Fig. 8). However, where r_e is calculated taking into account the presence of high concentrations of drops with diameters between about 50 μm and 1 mm, it continues to increase up to about 4 km (open triangles in Fig. 8). For cloud-sized droplets, our measurements indicate that a value of r_e of ~12–14 μm is required for the onset of an effective collision–coalescence process, compared to a threshold radius (i.e. $D_T/2$) of ~15–17 μm (see subsection 4(d)).

Figure 9 shows average droplet-size spectra at various heights above cloud base derived from measurements obtained on 24 August in 54 small cumulus clouds in regions where updraughts were likely to be prevalent (CLWC $\geqslant$0.3 g m^{-3}). The spectra are multi-modal, but there is a progression to larger drops with increasing height above cloud base. On this day, D_T was 35 μm at an average height above cloud base of ~1.3–1.5 km. All of the clouds that were sampled on this occasion that attained a depth of at least 1.3 km produced raindrops. The presence of multi-modal spectra can be attributed, in part, to sampling clouds at the same level in various stages of growth and dissipation.

(*c*) *Adiabaticity*

Figure 10 shows the 'adiabaticity', defined as the ratio of the measured CLWC to the adiabatic CLWC, for the non-raining and raining clouds that we studied in KWAJEX. The errors in the derived values of this ratio can be large near cloud base, where both the measured and adiabatic CLWC are small, and where fluctuations in cloud base height occur. None of the measurements of CLWC at >2 km above cloud base in raining clouds approached the adiabatic value, and at 5 km above cloud base the ratio of the measured values of CLWC to the adiabatic value was <0.1. These low ratios reflect the extraordinary efficiency with which CLWC is diluted by the conversion of cloud water to rain and by entrainment in these clouds.

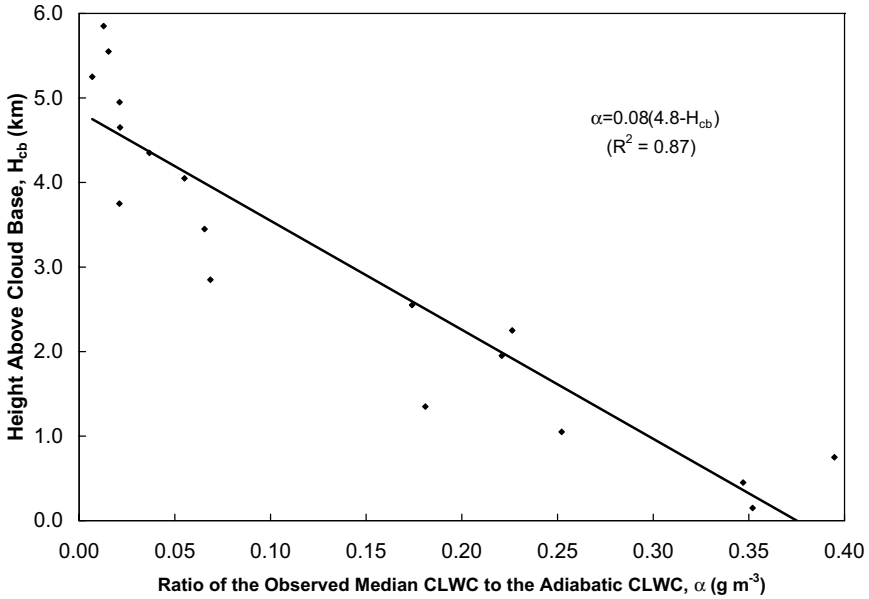

Figure 10. Ratio of median measured cloud liquid water content (CLWC) to the adiabatic CLWC, termed 'adiabaticity', for cumuliform clouds sampled from the Convair-580 aircraft in KWAJEX. The least-squares best fit is also shown.

(*d*) *Formation of rain by the collision–coalescence process*

Perhaps the most remarkable aspect of the clouds described here is the ease with which they rained. All clouds that exceeded 1.5 km in depth contained rain or drizzle drops. By the time the cloud tops reached 3–4 km amsl they regularly produced drops >5 mm diameter and heavy, very localized rain showers. Equally heavy rain, but usually in much larger rain shafts that reflected their greater girths, fell from all convective clouds that reached above ~4–5 km amsl (depths >4 km).

Figure 11 shows the relationship between the depth of the subset of 185 small to moderate sized convective clouds and the concentration of precipitation-sized particles ($\geqslant$100 μm maximum dimension). The concentration of these particles is well predicted by a least-squares best-fit to the data ($R^2 = 0.8$). Figure 11 shows that when cloud depths reached ~1 km the maximum concentration of precipitation-sized particles increased rapidly as the cloud depth increased to ~5 km, but thereafter increased more slowly.

Associated with the development of precipitation-sized drops was the broadening of the droplet spectra with height above cloud base. Figure 12 shows the relationship between the maximum value of D_T and the concentration of precipitation-sized particles. These measurements show that only after D_T reached >35 μm did precipitation-sized particles appear in measurable concentrations (~0.01 litre^{-1} as measured by the PMS 2D-C probe).

(*e*) *Variation of aerosols in the sub-cloud marine boundary layer and their effects on clouds and rain*

During KWAJEX, the visibility in the marine boundary layer varied from 'unrestricted' (cumulonimbus anvils that were barely above the horizon could be seen clearly on such days) to <30 km in relatively turbid, hazy conditions. Day-to-day changes in visibility at remote oceanic locations are thought to be due primarily to large

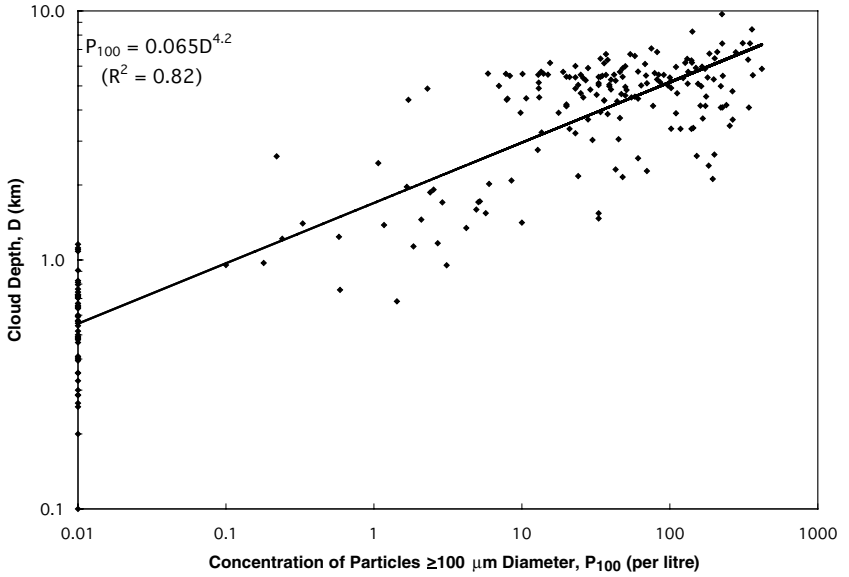

Figure 11. Cloud depth (km) versus concentration of precipitation-sized particles (litre^{-1}), i.e. particles $\geqslant 100$ μm in maximum dimensions, for cumuliform clouds sampled from the Convair-580 aircraft in KWAJEX. Growth of drops by the collision–coalescence process begins at cloud depths of $\sim$1.5 km. The concentration of precipitation-sized particles that were below measurable values (i.e. <0.01 litre^{-1}) are arbitrarily located at a concentration of 0.01 litre^{-1}. The least-squares best fit is also shown.

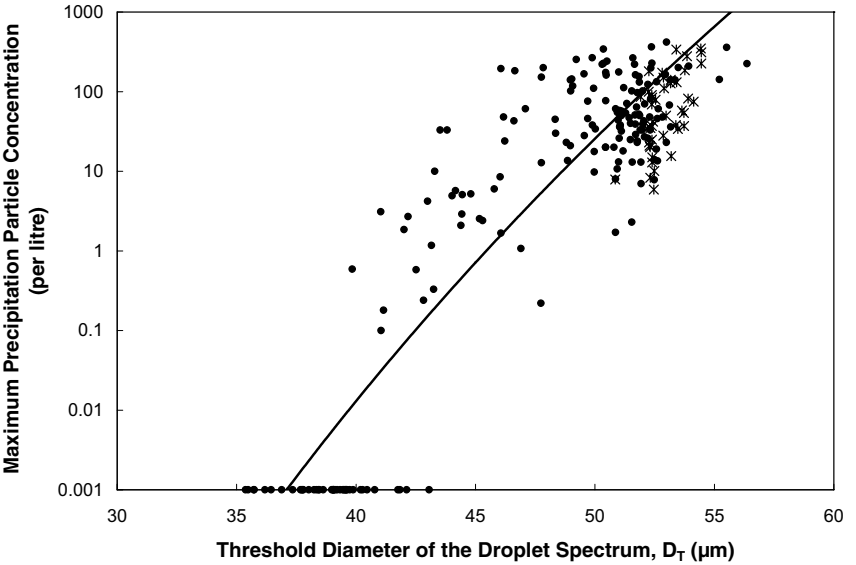

Figure 12. Maximum threshold droplet diameter (μm) of cloud drops versus concentration of precipitation-sized particles (litre^{-1}), i.e. particles $\geqslant 100$ μm in maximum dimensions, sampled from the Convair-580 aircraft in cumuliform clouds in KWAJEX. The concentrations of precipitation-sized particles that were below measurable values (i.e. <0.01 litre^{-1}) are arbitrarily located at a concentration of 0.001 litre^{-1}. Those concentrations comprising ice particles are denoted by asterisks.

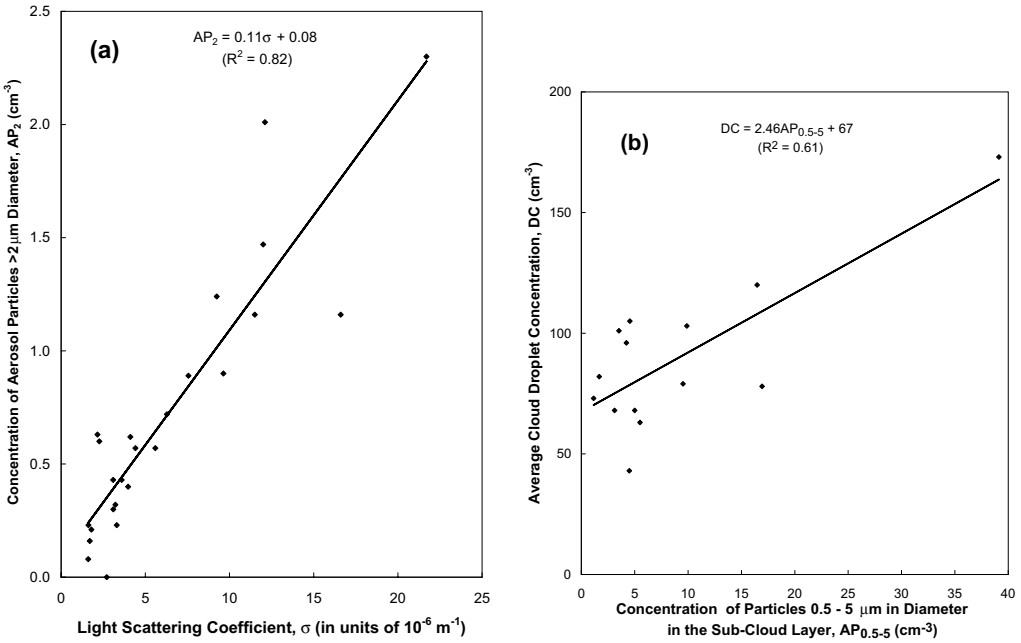

Figure 13. Using particle measurements made from the Convair-580 aircraft in KWAJEX in non-precipitating areas between the cloud base and ~100 m of the sea surface: (a) light-scattering coefficient at a wavelength of 550 nm versus concentration of aerosol particles >2 μm diameter; (b) concentration of particles 0.5–5 μm diameter versus average cloud droplet concentration. In both cases the least-squares best fit is also given.

particles raised by the wind from the ocean surface (e.g. Mordy and Eber 1954; Smith *et al.* 1993). However, these changes are usually not great enough to be reported by official observing stations, since the degradation of visibility does not normally lower it to below 10 km, where an 'obstruction' is required to be reported in official weather reports. Moreover, there are usually no distant objects within view at remote island locations to detect changes in longer-range visibility. Hence, subtle changes in visibility produced by changes in aerosol concentration are generally not found in the official observing records. Nevertheless, variations in sub-cloud-layer visibility from day to day, and on one day from one area to another less than 100 km away, were very evident in KWAJEX.

Table 2 summarizes the aerosol measurements in the sub-cloud marine boundary layer made aboard the Convair-580 in KWAJEX. Aerosol particle concentrations varied by more than an order of magnitude in the 17 days on which the Convair-580 flew. The largest sub-cloud aerosol particles detected (>2 μm diameter), though low in concentration, were well correlated ($R^2 = 0.8$) with visibility as represented by the light-scattering coefficient (Fig. 13(a)), as predicted by Kunkel (1984). The concentrations of the larger sub-cloud particles were also moderately correlated ($R^2 = 0.6$) with the average droplet correlations in the clouds overhead (Fig. 13(b)). The concentrations of sub-micron particles were uncorrelated with cloud droplet concentrations ($R^2 < 10^{-4}$) and with visibility (not shown). Our measurements do not show any marked effects of aerosols in the sub-cloud layer on the height above cloud base at which growth of cloud drops by the collision–coalescence process was initiated (i.e. ~1.5 km).

TABLE 2. SUMMARY OF AEROSOL CONDITIONS ENCOUNTERED AT KWAJALEIN, MARSHALL ISLANDS DURING KWAJEX JULY/AUGUST 1999

Date	A	B	C	D	E	F	Comments
25 July	1783	12.10	360	950	39.0	1.9	Low visibility; whitecaps present.
28 July	1784	2.65	380	300	5.0	0.5	High visibility; near calm conditions; no whitecaps.
30 July	1785	1.62	450	–	3.1	0.2	Light, variable winds. No whitecaps. Tremendous horizontal visibility at the surface (~180 km).
1 Aug	1786	3.51	340	–	5.5	0.5	–
3 Aug	1788	2.00	50	240	4.6	0.6	–
6 Aug	1789	7.29	185	410	16.5	0.1	Most haze since the beginning of project.
9 Aug	1791	12.50	41	300	16.9	1.6	Considerable low-level turbidity.
11 Aug	1792	1.80	188	–	1.2	0.2	–
23 Aug	1793	5.30	85	450	6.4	1.0	Noticeably hazy; numerous whitecaps; estimated wind speed ~7–12 m s^{-1}.
24 Aug	1794	3.34	154	280	4.2	0.5	Excellent visibility (~70 km); trace of salt haze visible.
25 Aug	1795	8.11	167	220	9.9	0.9	One of the windiest days and lowest visibilities in KWAJEX.
26 Aug	1796	4.20	40	320	5.4	0.5	More turbid on this day than on 27 August.
27 Aug	1797	2.59	29	280	1.7	1.3	Moderately turbid day; light winds; no whitecaps. Visibility ~20–30 km.
28 Aug	1798	15.20	233	910	9.5	1.0	Seemed to be in the same turbid environment as 27 August (although departed from Kwajalein in high-visibility conditions).
30 Aug	1799	3.47	32	210	4.5	0.9	Moderately hazy day.
	Average	5.71	182	406	9	0.78	
	Median	3.51	167	300	5	0.62	
	Standard deviation	4.38	142	255	10	0.52	
	Maximum	15.20	450	950	39	1.91	
	Minimum	1.62	29	210	1	0.11	

A. University of Washington flight number.
B. Average light scattering coefficient ($10^{-6}m^{-1}$) at wavelength $\lambda = 0.44$ μm in the sub-cloud layer.
C. Average concentration (cm^{-3}) measured by Particle Measuring System's Passive Cavity Aerosol Spectrometer Probe in the sub-cloud layer.
D. Average condensation nucleus concentration (cm^{-3}) in the sub-cloud layer.
E. Average concentration (cm^{-3}) of particles 0.3–20 μm in diameter in the sub-cloud layer.
F. Average concentration (cm^{-3}) of particles 2–47 μm diameter in the sub-cloud layer.

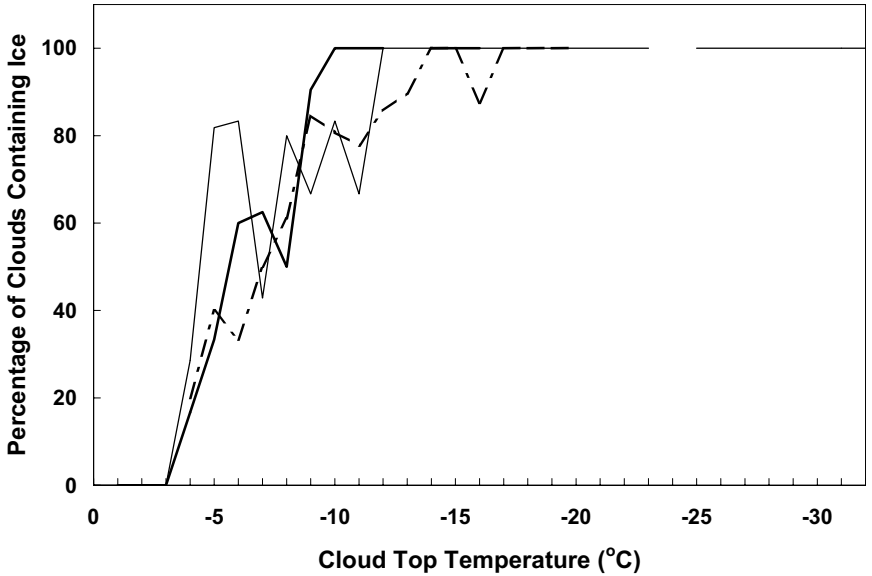

Figure 14. Percentage probability of intercepting ice particles in ageing or dissipating cumuliform clouds with top temperatures below 0 °C in KWAJEX (heavy solid line). Corresponding results are also shown for stratiform clouds in the Arctic boundary layer (light solid line) and cumulus clouds in Washington State coastal waters (dashed line).

(*f*) *The formation of precipitation via the ice process*

The concentrations of ice particles at temperatures between the freezing level and −10 °C were often extraordinarily high in the larger convective complexes encountered in KWAJEX. In this temperature range the concentrations of columnar ice crystals (consisting mainly of hollow sheaths and needles) usually exceeded 100 litre^{-1}, and the total concentration of ice particles, including irregular particles such as fragments, occasionally approached 1000 litre^{-1}, the highest concentrations of natural ice particles ever observed by us in many field studies. In contrast, rising cloud turrets whose tops had just passed through the −4 °C level were usually ice-free. Figure 14 shows the percentage of occasions on which ice particles were intercepted, as a function of cloud top temperature. Ice began to appear at cloud top temperatures of about −4 °C, and was virtually guaranteed for cloud top temperatures below about −10 °C, even in newly risen turrets. In KWAJEX, as in other locations, the maximum concentration of ice particles that appeared in a cloud was not well correlated with cloud top temperature. Rather, there was a sudden onset of ice (first stage), followed immediately by a second, prolific ice-forming stage that produced ice particle concentrations of hundreds per litre (Rangno and Hobbs 1991).

The first ice particles that appeared in such turrets, amid supercooled droplets, were frozen drops (some fragmented), graupel, and irregular ice fragments; some of the irregular ice fragments clearly originated from drops that had disintegrated on freezing. Measurements obtained on 30 August 1999, in one of the more vigorously ascending cumulonimbus calvus turrets that we sampled, provide data on the first stage of ice formation. Figure 15 shows a time line of some of the airborne measurements through this cloud. Note the increase in altitude of the aircraft after it entered the cloud (Fig. 15(a)), which was caused by the updraught encountered. We estimate conservatively that the updraught ranged from ∼5–10 m s^{-1}. Therefore, the cloud top

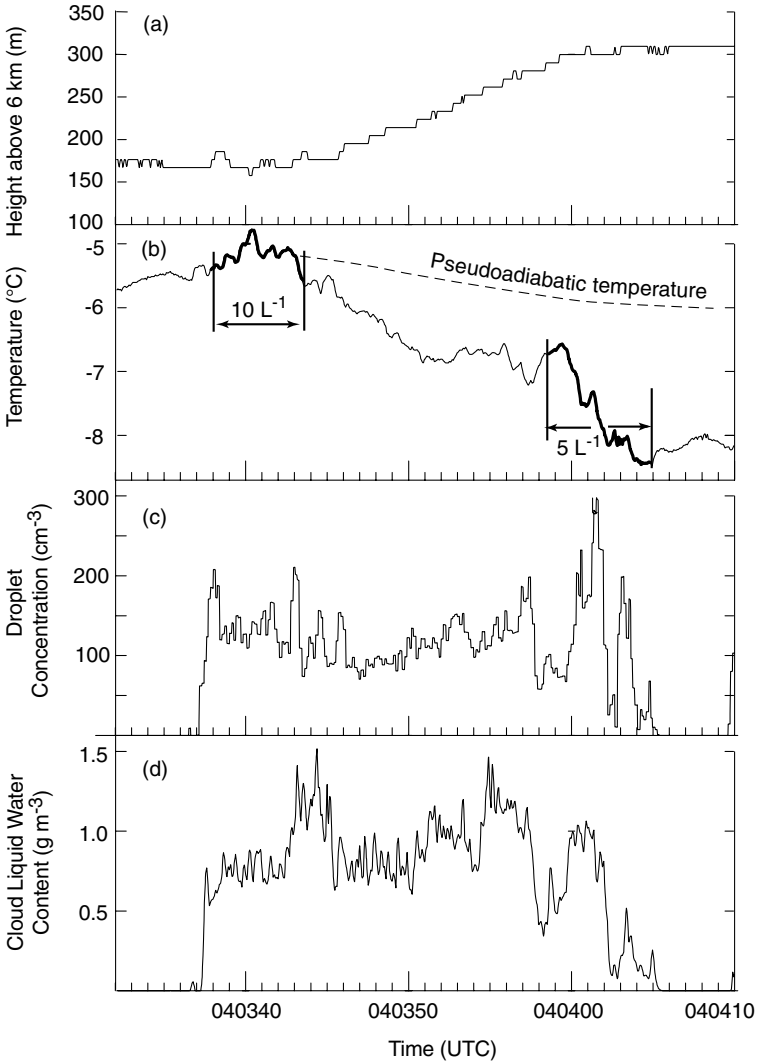

Figure 15. A time-line of measurements on 4 August 1999 from the Convair-580 aircraft in KWAJEX, 700 m below the top of a rising, pileus-capped cumulonimbus calvus cloud: (a) height of aircraft above 6 km amsl; (b) air temperature (continuous line), with regions where ice was detected indicated by thicker lines with average ice particle concentrations noted (litre^{-1}); (c) cloud droplet concentration; (d) cloud liquid water content.

is likely to have ascended through the freezing level ~170–340 s before the aircraft entered the cloud, and the cloud top passed through the −5 °C level ~100–200 s prior to cloud entry.

Figure 15(b) shows that during the initial 6 s of the cloud penetration the temperatures were greater than ambient. However, the temperature fell rapidly throughout the remaining 23 s of the cloud penetration, and at a rate considerably greater than the decrease in the pseudo-adiabatic temperature (dashed line in Fig. 15(b)) associated with a 115 m increase in altitude. This suggests that evaporative cooling due to cloud top and/or lateral mixing of dry ambient air had penetrated a large portion of the cloud. Ice particles, consisting either of ice fragments, columnar crystals, or graupel, were found in two dichotomous locations (denoted by the heavier portions of the curve in

Figure 16. All of the ice particles imaged by the cloud particle imager (CPI) in a sample volume of ~10 litres during a cloud penetration at an average temperature of −6 °C in a rapidly rising cloud turret on 30 August 1999, by the Convair-580 aircraft in KWAJEX. The cloud top temperature was −12 °C.

Fig. 15(b)): the first during the initial 7 s of the penetration, and the second during the last 8 s when the in-cloud air temperature was markedly lower. In these two regions, the concentrations of ice particles reached tens per litre over ~120 m (1 s) segments of the cloud. Close-up views of all the ice particles imaged by the CPI in a sampling volume of ~10 litres during the aircraft penetration of this young turret are shown in Fig. 16.

(*g*) *Types of ice particles*

Most of the regular ice particles encountered in convective regions by the Convair-580 in KWAJEX were hollow sheaths and needles, which grow at temperatures between −4 and −8 °C. There were also frozen drops (Fig. 17(a)), frozen or freezing drops with spicules (Fig. 17(b)), and ice fragments (Fig. 17(c)). The fragments were likely to have been pieces of frozen drops, bits of rime broken off from the many rimed ice particles and broken crystals. Appreciable CLWC (>0.3 g m^{-3}) sometimes coexisted with high concentrations of ice particles. This suggests that the high concentrations of ice had formed explosively in the previous few minutes. Also present were numerous frozen drops with sheath extensions, or what otherwise appeared to be complete sheaths with large (>30 μm) single drops apparently rimed on one end of the sheath (Fig. 17(b)).

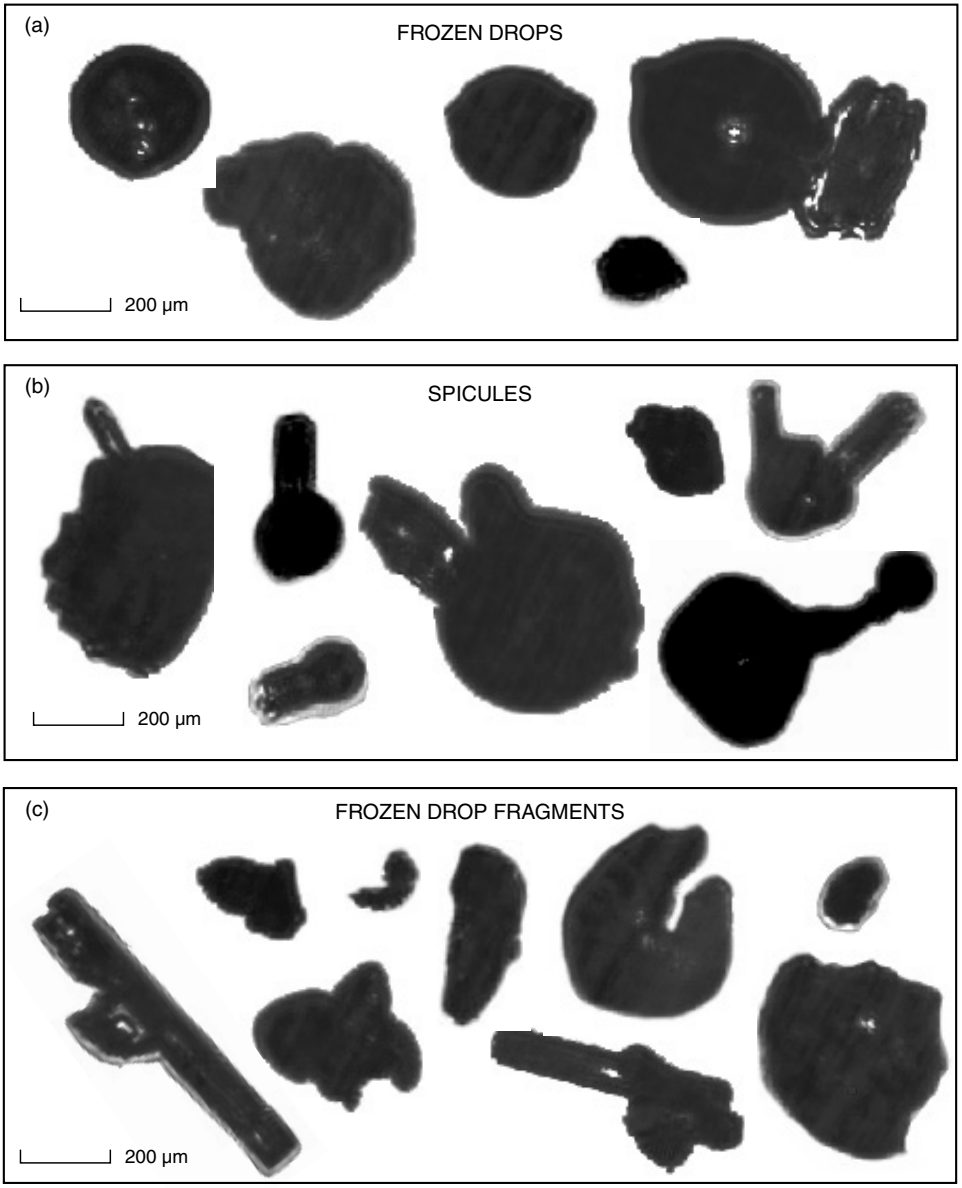

Figure 17. Examples of the ice particles encountered between −3 and −10 °C by the Convair-580 aircraft in KWAJEX during the first and second stages of ice formation: (a) frozen drops, (b) spicules, and (c) fragments of frozen drops.

The CPI and 2-DC imagery suggested that drop fragmentation during freezing was clearly part of the initial stage of ice formation. As mentioned previously, Fig. 16 shows all of the ice particles imaged by the CPI in a sample volume during an aircraft penetration of a vigorously rising, pileus-capped cumulonimbus calvus cloud on 30 August 1999. The average temperature at the level of penetration was −6 °C, and the tops of the cloud were just reaching the −12 °C level. The ice particles were either graupel or ice fragments >50 μm in maximum dimension. As can be seen from Fig. 16,

no columnar ice particles were imaged by the CPI. Only about 50 columnar ice particles were imaged by the PMS 2-DC probe in this 3.5 km length pass (sampling volume ~38.5 litres), even though the formation of ice was well underway. Hence, most of the very numerous micrometer-sized ice particles are likely to have been ejected during riming, and drop freezing had not yet reached the CPI-detectable sizes of ~20–40 μm at the time the aircraft passed through this cloud. This is consistent with the fact that the cloud top had passed through the −5 °C level about only 2 to 3 minutes prior to penetration by the aircraft.

5. Discussion

(*a*) *Overall cloud properties*

Clouds over the warm pool of the tropical Pacific Ocean have microstructures characteristic of pristine oceanic clouds far removed from anthropogenic sources of particles, namely: low droplet concentrations and a propensity to precipitate when only moderately deep. For example, in KWAJEX droplet concentrations averaged <100 cm^{-3}, and rain began to fall from the clouds when they were <2 km thick. Since there have been no comparable studies of small to medium-sized maritime cumulus and cumulonimbus clouds with cloud base temperatures as high as those reported here, in the following subsection we use our data to examine precipitation mechanisms in such clouds.

(*b*) *Onset and production of rain by the collision–coalescence mechanism*

The collision–coalescence process in clouds is ubiquitous, occurring in numerous marine and continental locales. For example, the collision–coalescence process has been documented in Arizona, Montana, and New Mexico in summer (MacCready and Takeuchi 1968; Harris-Hobbs and Cooper 1987; Blyth *et al.* 1997; Phillips *et al.* 2001), in Colorado in winter storms (Rasmussen *et al.* 1995), in Israel (Rangno 1988) and in South Africa (Mather *et al.* 1986). The collision–coalescence process also operates in deep, warm-based cumulus and cumulonimbus clouds in continental locations, such as the eastern half of the United States (Byers 1952; Koenig 1963; Braham 1964; Musil and Smith 1990; Changnon 1991; Herzegh and Jameson 1992), and has been inferred to operate throughout the western Pacific (Petty 1999).

The concentrations of precipitation-sized drops in KWAJEX increased rapidly with increasing cloud depth (Fig. 11). Combining this result with the linear relationship between cloud depth and cloud temperature (Fig. 2), we can infer a rapid increase in the concentration of precipitation-sized particles with decreasing cloud top temperature provided cloud base temperatures are relatively constant, which they are over the tropical Pacific Ocean. Thus, cloud top temperatures measured from satellites can be used to infer the concentrations of precipitation-sized particles in small to moderately sized convective clouds with tops near the freezing level that are located over the warm pool of the tropical Pacific Ocean.

The effective radius of cloud droplets is a useful parameter in discriminating precipitating from non-precipitating clouds via remote measurements (e.g. Rosenfeld and Gutman 1994; Rosenfeld and Lensky 1998). The *in situ* measurements of r_e reported here confirm this conclusion and also the modelling results of Khain *et al.* (2000) and Pinsky and Khain (2002). Our results show that the r_e must exceed ~12–14 μm for precipitation particles to form. However, r_e is not as good a predictor of the concentration of raindrops as are cloud depth, cloud top temperature, or the threshold droplet diameter. This is not surprising, since r_e is a broad measure of the characteristics

of the droplet spectrum, while D_T, for example, measures how many drops are likely to be involved in rain formation. The growth of the largest cloud drops, as represented by D_T, has nearly the same slope with increasing cloud depth for cumulus congestus and small cumulonimbus calvus in KWAJEX, as in the Azores and Washington State coastal waters (Fig. 7). This suggests that the same relationship may hold over large areas of the oceans.

Our measurements show that so much rain fell from moderately sized cumuliform clouds in KWAJEX that their CLWCs began to decline when cloud depths exceeded 2–3 km (Fig. 6). Drops as large as 5 mm in diameter were sometimes present in clouds no deeper than 2–3 km over the warm pool of the tropical Pacific Ocean. On one occasion in KWAJEX (25 July 1999) we measured one of the largest raindrops ever observed, which had a maximum dimension of at least 8.8 mm (Hobbs and Rangno 2004), from a cloud with a top near the freezing level. Similarly sized drops have been reported in shallow cumulus clouds over Hawaii, but with cooler cloud bases (18 °C; Beard *et al.* 1986).

Saunders (1965) reported that rain in the Bahamas could develop from fractocumulus clouds that grew into tall cumulus in ~25–35 minutes. He also noted that extreme rain rates of 100 mm h^{-1} had durations of only ~1–2 minutes. Rauber *et al.* (1991) hypothesized that giant drops (3–8 mm in diameter), which might comprise such rain, formed in short-lived water-rich updraughts. This scenario, which was postulated to explain the large drops observed by Beard *et al.* (1986) in Hawaii, might also explain the short durations of extremely heavy rainfall observed by Saunders in the Bahamas, and our own observations in KWAJEX of filamented shafts of rain, only tens to a few hundreds of metres in width, that contained drops >5 mm in diameter falling from clouds with tops that did not reach the 600 hPa pressure level (see subsection (h) below).

Saunders' radar data is probably also representative of clouds over the warm pool of the tropical Pacific Ocean, since all clouds that reached ~4 km amsl (i.e. ~3.5 km thick) in KWAJEX precipitated heavily. To reach this depth with a ~3–5 m s^{-1} updraught from cloud base (500 m amsl) to 4 km amsl would take only ~12–19 minutes. Therefore, we infer that the time to produce heavy rain via the collision–coalescence process in the clouds of the Pacific warm pool is <12–19 minutes. For a cloud to reach a depth of 1.5 km (i.e. about the minimum depth to ensure rain in KWAJEX) would take only ~5–10 minutes.

Saunders (1965) reported that in the Bahamas there was not much change in rain intensity with increasing cloud depth once a cloud attained a depth of about 4 km, even if it subsequently grew to a depth of 15 km. Since clouds 4 km deep in the Bahamas are all liquid and clouds 15 km deep certainly contain ice, it appears that the presence of ice in deeper clouds contributes little to rain intensity in the Bahamas. Figure 18 shows average and median rain rates, derived from several of the airborne instruments in KWAJEX, for clouds with tops above and below 0 °C. It can be seen that the heaviest rain from the all-liquid clouds was similar to that from those clouds whose tops extended far above the 0 °C level. This supports the inference that ice contributes little to rain intensity in tropical maritime convective clouds (stratiform regions of ice-producing clouds were avoided in the derivation of rain rates by considering only those rates ⩾25 mm h^{-1}). However, because of their much greater horizontal extents, the total precipitation from clouds that extended upwards to well below freezing temperatures was, of course, considerably greater than that from clouds that did not contain ice. Even so, most of the precipitation-sized ice particles in the deep isolated convective clouds sheared away from the lower convective body of the cloud and evaporated into dry air below. In contrast, the warm cumulus clouds did not disperse cloud material

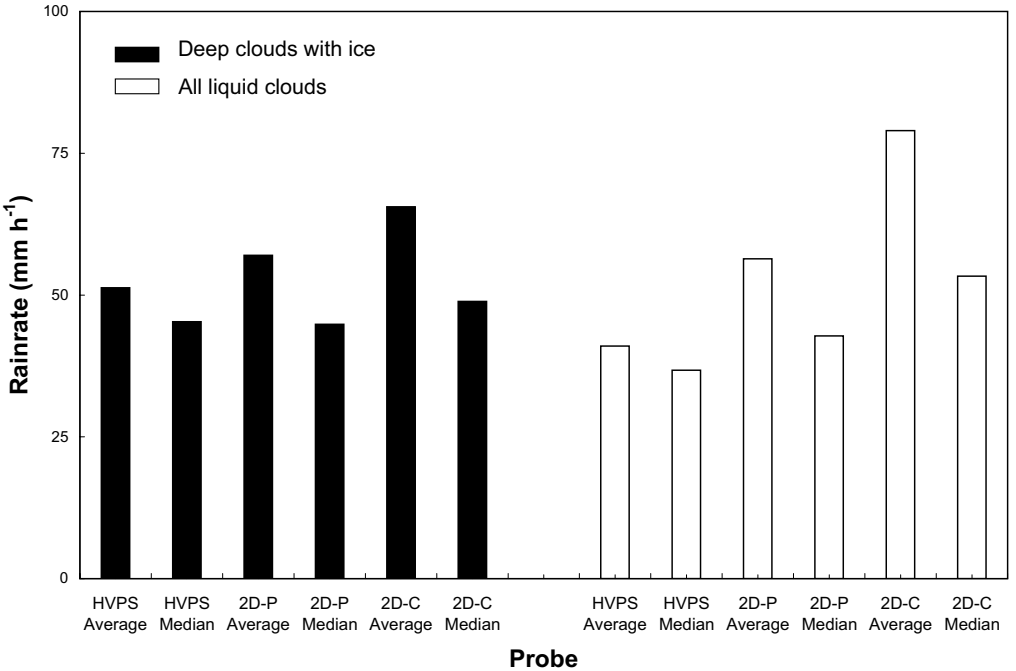

Figure 18. Comparisons of average and median instantaneous rain rates ($\geqslant$25 mm h^{-1}) at 800 hPa in convective clouds measured from the Convair-580 aircraft in KWAJEX. Clouds containing ice particles (shaded) and those entirely of liquid water are shown separately. Measurements were by: Stratton Park Engineering Company high-volume precipitation sampler (HVPS), Particle Measurement Systems (PMS) 2D cloud probe (2D-C), and PMS precipitation probe (2D-P).

into anvils; therefore, their precipitation efficiency was probably greater than that of the deep convective clouds. The vast mesoscale cloud complexes with precipitating stratiform regions must also have low precipitation efficiencies, since much of the leading boundaries of the stratiform regions are middle- and high-level ice clouds that do not precipitate to the ground.

(*c*) *Microstructure of the liquid water clouds*

Ackerman (1963) found that the CLWC in tropical cumulus clouds began to decrease at heights above a pressure level of ~750 hPa. This is consistent with the measurements reported here, those made by Black and Hallett (1986) in hurricane rain bands, and by Stith *et al.* (2002) in KWAJEX. Ackerman (1967) observed that cumulus clouds exhibited preferred sub-cloud sizes; today we might say they are 'fractal-like'. From spectral analysis of cumulus liquid water contents, Ackerman deduced the presence of non-random fluctuations in cloud-scale motions with wavelengths that peaked at about ~280 and ~630 m. These scales appear to be confirmed by Austin *et al.* (1985) who found that the widths of cumulus updraughts averaged ~300 m. Austin *et al.* inferred, from droplet-size distributions, an additional preferred width of ~100–200 m. Figure 5 does not reveal a preferred width for liquid water clouds in KWAJEX, even though cumulus clouds are clearly fractal-like (e.g. Takaya 1993). However, an aircraft is unlikely to penetrate the sub-elements of a cumulus cloud one after the other, but will mostly sample the centres of some substructures while just grazing others.

(*d*) *Effects on cloud microstructure of aerosol particles in the sub-cloud layer*

Aerosols can have profound effects on the microstructures of clouds and possibly on the formation of precipitation (Gunn and Phillips 1957; Squires 1958a,b,c; Twomey 1959; Rosenfeld and Lensky 1998; Rosenfeld 2000). When the concentrations of cloud condensation nuclei (CCN), and therefore cloud droplet concentrations, are low and the droplet-size spectra are broad, raindrops can form fairly efficiently by the collision–coalescence process. When CCN concentrations, and therefore cloud droplet concentrations, are high, and the droplet-size spectra are narrow, the growth of drops of precipitable size is more difficult (e.g. Wallace and Hobbs 1977).

In KWAJEX, changes were observed in aerosol concentrations in the marine boundary layer even though intrusions of continental aerosols were not observed. However, the modest changes in aerosols that we observed did not appear to have any marked effects on precipitation production. This may have been because the concentrations of CCN at cloud levels were not greatly affected by the additional aerosols produced by enhanced whitecap activity on breezier days.

There is evidence that in less pristine locations than the Marshall Islands the initiation of 'warm rain' begins with a few large drops that form on ultra-giant CCN (>20 μm diameter; e.g. Johnson 1982, 1993; Caylor and Illingworth 1987; Illingworth 1988; Knight *et al.* 2002). In about 8 h of sampling the sub-cloud layer with the FSSP-100, we did not detect ultra-giant particles that might serve as centres for early raindrop formation (see subsection 4(e) and Table 2). We also examined the sub-cloud imagery from the CPI and 2D-C for large particles but did not find any. However, the total sample volume for all of these instruments during the 7.85 h of sub-cloud flying was less than 15 m^{-3}, which is rather small. There are also sampling biases: we did not fly very near the surface where large aerosol particles would likely be detected, particularly on days with numerous whitecaps, but rather flew mostly at the top of the sub-cloud layer; also, much of our flying was between disturbed areas. Hence, while we did not detect any 'ultra-giant' aerosol particles, they may have existed in low concentrations. The sizes and concentrations of raindrops formed a continuum, from a few >100 μm diameter drops formed by collision–coalescence to high concentrations of drizzle and raindrops as the cloud deepened. The first raindrops that formed in the small to moderate sized cumulus clouds were $\sim$100–500 μm in diameter or somewhat larger. Clouds from which drizzle drops and small raindrops began to fall were only $\sim$1–1.5 km in depth. However, with just another half-kilometre increase in cloud depth, drops >3 mm diameter were encountered. These results suggest that the initial droplet spectra at cloud base, combined with turbulence and the presence of zones of high CLWC, may be more important in the development of rain than ultra-giant aerosol particles, since we did not detect such particles (see, for example, Manton 1979; Khain *et al.* 2000; Pinsky and Khain 2002).

(*e*) *Origin of the ice particles*

It is well established that cumuliform clouds containing precipitation-sized drops (>100 μm in diameter) as they ascend to temperatures below 0 °C produce ice by the time they reach temperatures between about -4 and -10 °C (e.g. Koenig 1963; Mossop and Ono 1969; Mossop *et al.* 1970; Ono 1972; Hallett *et al.* 1978; Mossop 1985; Hobbs and Rangno 1985, 1990; Willis *et al.* 1994; Jameson *et al.* 1996; Yuter and Houze 1998; Zeng *et al.* 2001). Similar observations were made in KWAJEX. The first ice particles to form in the clouds we studied derived from the freezing of isolated drops. Some such drops shattered during freezing to produce fragments (Fig. 17(c)), which

either slightly preceded or accompanied the appreciable growth of the first round of ice splinters shed by graupel particles. The freezing of some drops, and their subsequent conversion to graupel accompanied by splinter production during riming, produced massive concentrations of small ice particles and rapid glaciation of cloud turrets.

The fragmentation of individual drops during freezing has been studied extensively in the laboratory (e.g. Mason and Maybank 1960; Dye and Hobbs 1966, 1968; Brownscombe and Hallett 1967; Hobbs and Alkezweeny 1968; Johnson and Hallett 1968; Kolomeychuk *et al.* 1975; Pruppacher and Schlamp 1975). The fragmentation of individual precipitation-sized drops during freezing has mainly been observed to occur from −3 to −8 °C and when the drops freeze roughly symmetrically inwards, so that an ice shell encloses a liquid centre that expands on freezing (Dye and Hobbs 1968; Johnson and Hallett 1968). Pitter and Pruppacher (1973) and Pruppacher and Schlamp (1975) observed that drops begin to tumble in free fall as they freeze; this can permit symmetric freezing and shattering. However, until now the evidence for the fragmentation of freezing drops in clouds has been meagre (e.g. Knight and Knight 1974; Rangno and Hobbs 2001). The CPI imagery obtained in the present study provides strong evidence for the fragmentation of drops with diameters >50 μm (Fig. 17(c)). This size requirement was deduced from the rather large sizes of the fragments of frozen drops. It provides an independent field verification of the results of laboratory experiments on the freezing of drops in free fall, in which it was observed that only those drops >50 μm fragmented (Hobbs and Alkezweeney 1968). The ice particles produced by such fragmentation have been shown to accelerate the formation and spread of ice in clouds, particularly when combined with concomitant ice splinter production during riming (e.g. Chisnell and Latham 1976).

(*f*) *Rapidity of ice development*

The maximum concentrations of ice particles that we measured in KWAJEX with the PMS 2D-C probe (~500–1000 litre^{-1} of particles >100 μm in maximum dimensions) were the highest that we have measured in numerous field studies in many locations. Conditions for ice splinter production during riming (Hallett and Mossop 1974; Mossop 1976) were always met in the cloud turrets that reached sub-freezing temperatures. For example, graupel formed by the freezing of drizzle or raindrops was always present in the turrets in the riming–splintering temperature zone (−2.5 to −8 °C) soon after the turrets rose above the −5 to −10 °C levels. Also, rimed frozen drops always appeared before, or were coincident with, high concentrations of small (<500 μm maximum dimension) columnar ice particles. The concentrations of drops >23 μm diameter, which laboratory experiments show are required for riming–splintering (e.g. Mossop 1985), were always plentiful, usually exceeding 10 cm^{-3} in young turrets that had just ascended to the riming–splintering zone. Therefore, it is likely that the riming–splintering mechanism made a major contribution to the high concentrations of ice particles in the convective turrets. In addition, there were many tens of drops of diameter >50 μm litre^{-1} in ascending turrets in this zone.

However, the fragmentation of isolated drops during freezing also contributed significantly to the ice particle concentrations. In modelling studies, Chisnell and Latham (1976), Scott and Hobbs (1977) and more recently Philips *et al.* (2001) incorporated the effects of ice fragments produced by the freezing of isolated drops in free fall. The Chisnell and Latham model predicted that the time required to produce an ice enhancement factor of 10^4 over primary ice nucleus concentrations of ~0.01 litre^{-1} at −10 °C (Fletcher 1962) was ~10–15 minutes. The use of more recent ice nucleus concentrations (Meyers *et al.* 1992) would reduce the time to produce a multiplication

factor of 10^4 to ~5–10 minutes; from our observations in KWAJEX we estimate a time period of <10 minutes. Thus, the Chisnell–Latham model, with moderate augmentation of splinter production during riming by drop shattering, could account for the rapid proliferation of ice seen in the KWAJEX cumulus turrets as they neared and rose above the −10 °C temperature level. The Scott and Hobbs model found that the ejection of one splinter per freezing drop doubled the concentration of graupel, while four splinters from a freezing drop could increase graupel concentrations by a factor of 100. Philips *et al.* (2001) also found in modelling simulations that the fragmentation of freezing drops significantly increased ice concentrations without any other mechanisms at work. It appears, therefore, that the fragmentation of isolated drops during freezing, combined with splinter production by riming, can account for the rapid formation of very high concentrations of ice particles found in these clouds.

The average concentrations of drops >23 μm diameter in the Hallet–Mossop temperature zone are about three times higher (33 cm^{-3}) in polar maritime clouds in onshore flow off the Washington coast than the average concentrations of these drops (12 cm^{-3}) in the cumuliform clouds of KWAJEX. In KWAJEX, the Hallett–Mossop temperature zone is located about 4.5 km above cloud base, and much of the cloud water and larger drops are removed by the warm-rain process before reaching this temperature zone. This is likely to account for comparable glaciation rates in clouds in quite different locations. Average concentrations of graupel of 1 mm and larger in the Hallett–Mossop temperature zone in KWAJEX were 0.5 $litre^{-1}$; in the Washington maritime clouds these concentrations were ~0.3 $litre^{-1}$. The graupel concentrations in KWAJEX clouds in the Hallett–Mossop temperature zone are about one-tenth of those in Florida cumulonimbus clouds (e.g. Hallett *et al.* 1978), as are the concentrations of supercooled millimetre drops. These observations support the view that in KWAJEX most of these particles are 'rained out' well before they reach the Hallett–Mossop temperature zone. Consequently, in these clouds the Hallett–Mossop mechanism would not be expected to operate as efficiently as in, say, Florida. This suggests that the relative inefficiency of the Hallett–Mossop mechanisms in the KWAJEX clouds was compensated by the fragmentation during freezing of isolated drops >50 μm in diameter.

Another intriguing observation in KWAJEX was the frequent observation of sheath ice crystals with a single frozen drop on their ends. This suggests that these particles were originally spicules that grew by vapour deposition as sheaths or columns (Fig. 17(b)). Usually such configurations would be viewed as single drops that collided with one end of a columnar crystal and then spread on impact (e.g. Mosimann *et al.* 1994). However, the transformation of a frozen droplet with spicules to crystalline ice was observed by Magono *et al.* (1979), Ohtake *et al.* (1982) and Sato and Kikuchi (1989). In KWAJEX, frozen drops with spicules were often found in regions where the air was saturated with respect to water (thus supersaturated with respect to ice), and vapour deposition was therefore likely to be greatest on protuberances such as spicules.

Plume-like regions of high concentrations of ice particles were encountered in cloud turrets during KWAJEX (Fig. 19(a)). These regions were ~1–2 km across, with well-defined boundaries, rather like newly risen smoke plumes containing high concentrations of small particles from a hot fire. Surrounding regions of lower and more uniform ice particle concentrations were diffuse (Fig. 19(b)) and composed of aggregates, like old stratified smoke plumes. The compact regions of high concentrations of ice particles resembled the explosive second stage of ice formation discussed by Hobbs and Rangno (1990) and Rangno and Hobbs (1991), which resembled cloud seeding with dry ice. Following the second, explosive stage of ice formation, ice particle concentrations

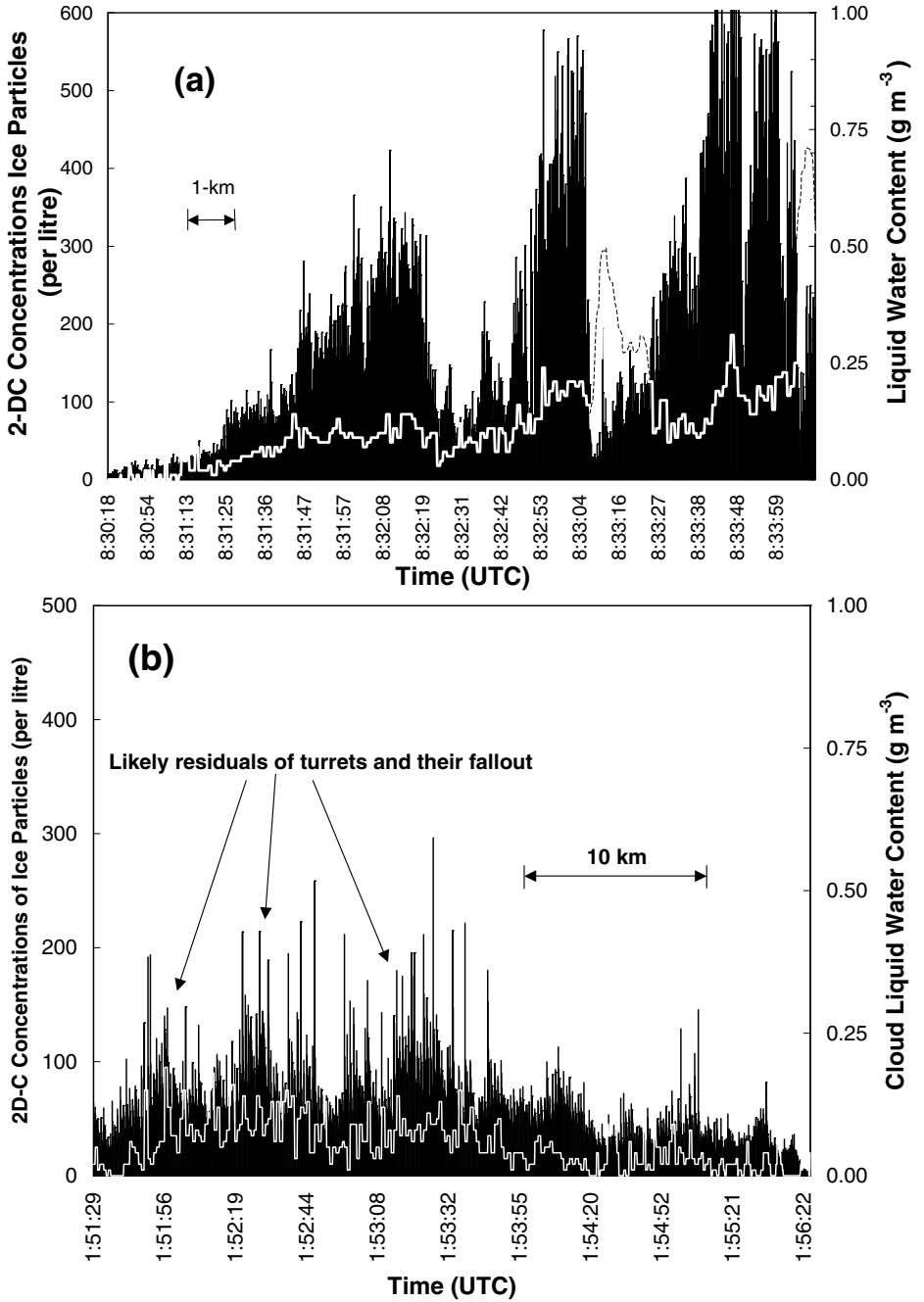

Figure 19. Concentrations of ice particles measured from the University of Washington Convair-580 aircraft in KWAJEX: (a) in an example of regions of newly formed, small ice particles at −6 °C; the sharp peaks in ice particle concentrations (black vertical lines from Particle Measurement Systems (PMS) 2D cloud probe (2D-C) records) suggest young 'plumes'; and (b) in an example of an ageing, stratiform region of larger ice particles and aggregates. The lower and more uniform concentrations in (b) compared to (a) suggest an older stratified plume. Note the difference in the scales used for the left-hand ordinates in (a) and (b). The white curves show the cloud liquid water content, and that in (a) is dashed between regions with high concentrations of ice particles.

decreased due to aggregation, fallout, and dispersion into anvils. No new ice particles appeared to form once the CLWC was depleted.

To recap: in KWAJEX the first ice particles that appeared in cloud turrets were graupel, frozen drops, columns and ice fragments (e.g. Fig. 17); such young turrets were low in concentrations of columnar ice particles, even though the aircraft flew mainly where columnar crystals should form (−4 to –8 °C). In the second stage of ice formation, high concentrations (>100 s litre^{-1}) of very small columns appeared very rapidly. Most of these columns were 100–500 μm in maximum dimension (suggesting formation times of <500 s). There were very few or no ice aggregates at this time. In spite of the high concentrations of ice particles, some CLWC was usually present. Graupel was usually still present in the second stage of ice formation. The small crystal sizes, and the presence of CLWC and graupel, all suggest very recent and very sudden ice formation.

To pursue this further, we evaluated 17 periods (for a total of 333 s of flight time) from four of our flights in KWAJEX in which both 2D-C cloud measurements and CPI imagery were available, in order to evaluate the types of ice particles that formed so quickly in regions like the ones described above. Figure 20 shows a typical region with a high concentration of newly formed ice particles that we examined. Figure 21 shows the size spectra of the three types of small ice particles observed with the CPI in the 17 periods: frozen drops (Fig. 21(a)), ice fragments (Fig. 21(b)), and columnar crystals (Fig. 21(c)). To our surprise, there was a pronounced lack of small columns below about 100 μm in maximum dimension, compared with the concentrations of ice fragments and frozen drops. Since the Hallett–Mossop criteria for splinter production was always met in these clouds, and splinters start out as fragments <10 μm in size (Bader *et al.* 1974; Choularton *et al.* 1978), they should grow into recognizable columns (needles or sheaths).

Why did we not observe many small columns when we flew in regions containing newly formed ice particles in the −2.5 to −8 °C temperature zone and with appreciable CLWC present? We propose two scenarios that might account for the deficit of small columns compared with similar-sized frozen drops and ice fragments. The first is that many of the micron-sized splinters produced at the onset of the Hallett–Mossop mechanism are swept up by cloud and precipitation-sized drops causing the drops to freeze before they can be seen with the CPI. Another possible scenario is that the freezing of many drops in the Hallett–Mossop zone is accompanied by a nearly direct transformation to crystalline ice shortly after the production of spicules (e.g. Fig. 17(b)). The spicules then become favoured sites for vapour deposition. Blanchard (1951) reported that it took only 8 s for a fully formed spicule to emerge from a freezing raindrop. Magono *et al.* (1979), Ohtake *et al.* (1982) and Sato and Kikuchi (1989) observed a transformation of cloud drops with spicules to pristine crystals (with no indication of a drop origin) at temperatures below −15 °C in the Arctic. Perhaps a similar transformation occurs in clouds over the tropical Pacific Ocean.

(*g*) *Role of ice in producing precipitation in small and moderately sized cumulonimbus clouds*

Due to the prolific development of small ice particles in cumulonimbus turrets as they ascended to the −5 to −10 °C temperature zone, it is likely that ice particles above the −10 °C level that did not originate as frozen drops contributed little to precipitation at the ground in convective regions, but later contributed to virga and precipitation in large stratiform systems. In the moderately sized cumulonimbus clouds studied in KWAJEX, these turrets generally encountered wind shear at or above the freezing

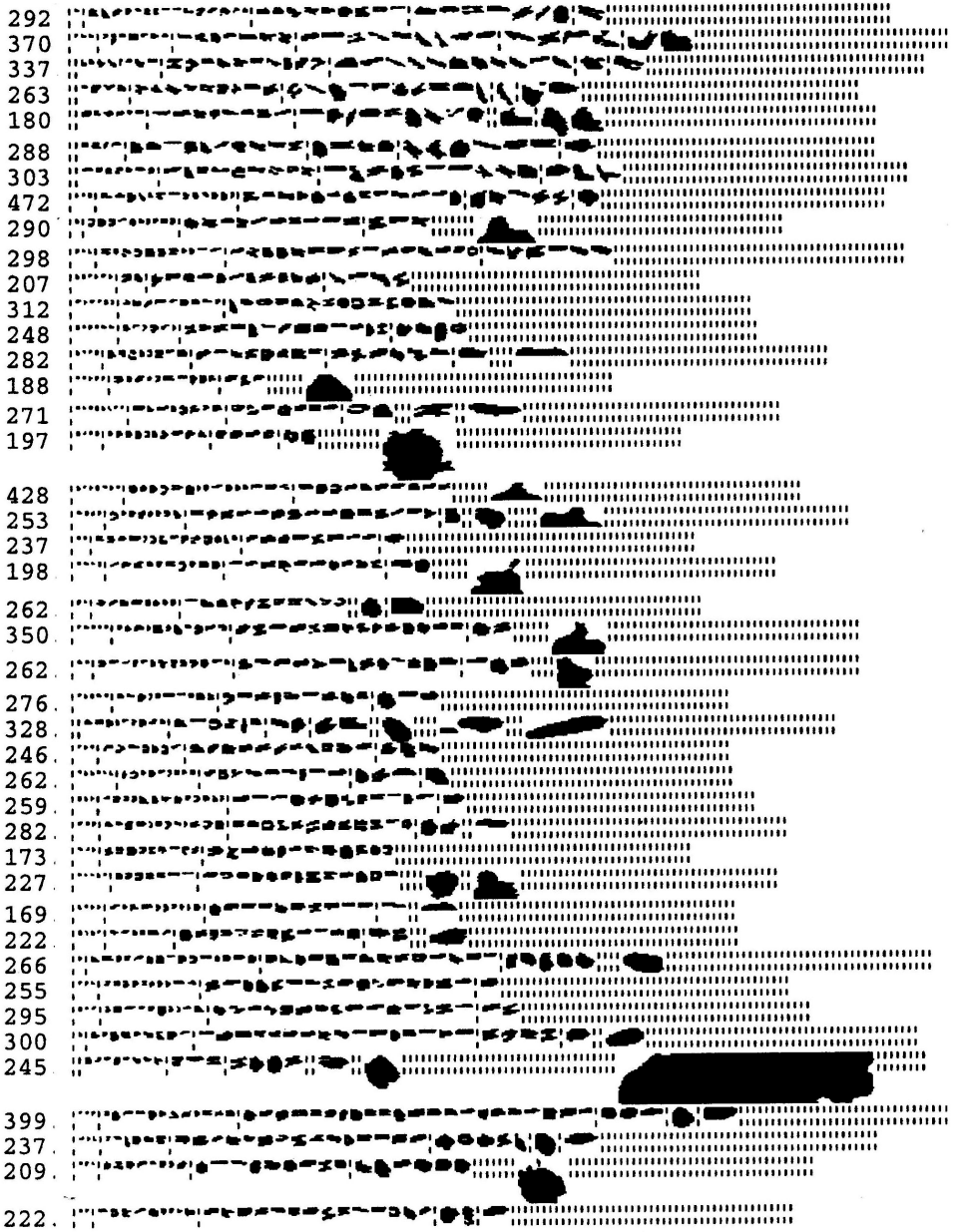

Figure 20. Example of high concentrations of newly formed ice particles frequently encountered by the University of Washington (UW) Convair-580 aircraft in KWAJEX. Numbers on the left are concentrations (litre^{-1}). Particle profiles are arranged in order of increasing size by 100 μm bins, separated by vertical double dashes. The greatest vertical extent of the largest particle shown is 800 μm. The measurements were made at −5.5 °C on 28 July 1999 (UW flight 1784) at 490 hPa between 082426 and 082434 UTC.

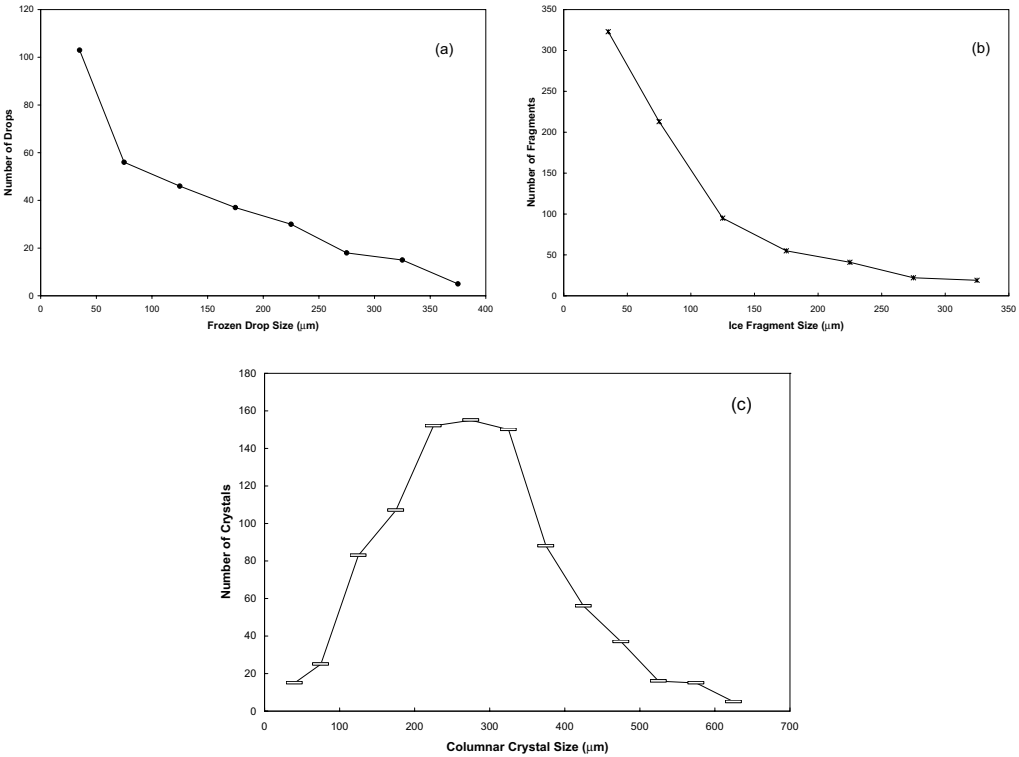

Figure 21. Size spectra of newly formed: (a) frozen drops, (b) ice fragments, and (c) columns. See text for details.

level, and the ice particles aloft were carried away in anvils. When the atmosphere was 'disturbed', deeply convective and moist, the anvil ice regions could cover thousands of square kilometres and produce light to moderate rain at the ground, even though the visual 'cloud bases' were ~5 km above sea level (i.e. at the freezing level). In smaller cumulonimbus clouds with modest updraughts (<10 m s^{-1}), of the type generally discussed in this paper, the high concentrations of ice particles often produced hard-appearing, tufted mounds, but little or no precipitation at the ground when they sheared away from the portion of the cloud that was below the freezing level.

(*h*) *Organization of large precipitation particles into vertical filaments*

Throughout the sampling of vigorous convective clouds in KWAJEX we observed bursts of precipitation on the pilot's window and on the hemispherical dome atop the aircraft fuselage. The durations of many bursts were only ~0.1–0.2 s, which suggests groupings of large particles (graupel or frozen drops) on horizontal scales of ~10–20 m. Particles capable of producing audible sound within the aircraft must have been several millimetres in diameter. Such large particles must have experienced especially favourable growth histories. This, in turn, suggests narrow channels of high CLWC above the levels where such particles were encountered, in which the ice particles grew quickly to large sizes by riming. Under appropriate conditions, and following the occurrence of graupel, the splinters produced by riming could produce localized regions of augmented ice enhancement (Rangno and Hobbs 1991). However, Rangno and Hobbs (1994) found that high concentrations of ice particles could form *in situ*

outside the Hallett–Mossop temperature zone for splinter production, by riming in a manner analogous to dry ice seeding.

In studies in other locales, we have associated bursts of large ice particles with vertical filaments or ice streamers (Hobbs and Rangno 1985; Rangno and Hobbs 1991). The filamented structure of young rain shafts below convective cloud bases is a common visual sight, as are filamented substructures in cirrus uncinus clouds and virga from altocumulus clouds. Vertically oriented 'streamers', or collections of strands, are also typical of 'generating cells' in regions of low wind shear (Plank *et al.* 1955).

Our observations of bursts of extraordinarily large raindrops and large graupel, located in vertical filaments, support the mechanism of formation of very large precipitation particles suggested by Rauber *et al.* (1991) and Szumowski *et al.* (1997). These researchers surmised that a few drops that descend within narrow channels containing above average liquid water content grow exceptionally fast. The low concentrations of such drops would make drop breakup through collisions with other millimetre-sized raindrops unlikely.

From Eq. (6.7) in Mason (1971), we have

$$\int_{R_1}^{R_2} \mathrm{d}R = \frac{E'\overline{w}(\overline{V} - v)}{4\rho_{\mathrm{L}}} \int_{t_1}^{t_2} \mathrm{d}t \tag{1}$$

where, R is the radius of a drop (m) growing by collision-coalescence from radius R_1 to R_2 in the time interval $t_2 - t_1$ (s), E' is the collection efficiency of the drop (dimensionless), $\overline{w}$ the average CLWC (g m^{-3}) through which the drop falls, $\overline{V}$ the mean fall speed of the drop (m s^{-1}) between radii R_1 and R_2, v the fall speed (m s^{-1}) of the much smaller droplets being captured by the growing drop, and ρ_{L} the density of liquid water (g m^{-3}). If $\overline{V} \gg v$, (1) becomes

$$(R_2 - R_1) = \frac{E'\overline{w}\overline{V}}{4\rho_{\mathrm{L}}}(t_2 - t_1).$$

Therefore, for a drop growing from an initial radius of, say, 0.0001 m (i.e. 0.1 mm) to a radius of, say, 0.0025 m (i.e. 2.5 mm radius or 5 mm diameter),

$$(0.0025 - 0.0001) = \frac{E'\overline{w}\overline{V}}{4\rho_{\mathrm{L}}}(t_2 - t_1). \tag{2}$$

Assuming $E' = 1$, $\overline{V} = 7$ m s^{-1} (i.e. the average fall speed of a drop with radii between 0.0001 m and 0.0025 m, obtained from Table B.1 in Mason (1971)), $\rho_{\mathrm{L}} = 10^6$ g m^{-3}, and $(t_2 - t_1) = 10$ minutes or 600 s (see subsection 5(a)), we have from (2)

$$\begin{aligned}\overline{w} &= \frac{(0.024)4(10^6)}{7(600)} \\ &= 2.2 \text{ g m}^{-3}.\end{aligned}$$

This value of $\overline{w}$ is about five times the average CLWC that was measured, and it is about 75–85% of the adiabatic CLWC in some of the shallow cumulus clouds (tops $\approx$ 800 hPa) that produced a few large drops. This suggests that regions of above average CLWC, referred to above, may correspond to pockets of nearly adiabatic CLWC.

Recently there have been several studies of the clustering of precipitation particles, and its effects on precipitation processes and the interpretations of radar data (Kostinski and Jameson 1997, 2000; Shaw *et al.* 1998; Jameson and Kostinski 1999). Pinsky and

Khain (1997, 2001) attributed the clustering of drizzle-sized drops to an inherent property of cumulus dynamics that organizes drops into clusters, a phenomenon they called 'self-concentration'. Their model results appear to be consistent with the observations reported here and those of Hobbs and Rangno (1985), of localized concentrations of drizzle drops and ice particles in filaments a few metres to tens of metres wide.

6. Conclusions

In this paper we have shown that precipitation is produced very efficiently by the collision–coalescence process in cumuliform clouds that form over the warm pool of the tropical Pacific Ocean in July and August, provided the depths of the clouds reach ~1.5 km. The concentration of raindrops within a few kilometres of cloud base is highly correlated with cloud depth ($R^2 = 0.8$). Since the cloud temperature is a linear function of altitude ($R^2 = 0.98$), and cloud base heights are relatively constant in the tropics, cloud depth and raindrop concentrations up to ~6 km amsl can be inferred from satellite measurements of cloud top temperature. The formation of rain begins when the concentration of drops >30 μm in diameter reaches ~3 cm^{-3}, or when the effective droplet radius reaches ~12–14 μm.

Adiabatic CLWCs were not observed. Above 3 km, the ratio of the measured LWC to the adiabatic value was usually <0.1, even in newly risen turrets. These low values of CLWC testify to the efficiency of the conversion of cloud water (drops <50 μm) to raindrops and of entrainment.

Ice particle formation was prolific at temperatures between about −3 and −10 °C, often reaching >500 litre^{-1}. The ice particles in established cumulonimbus clusters were comprised primarily of sheaths, needles and irregular ice fragments. The high concentrations of ice were initiated by the freezing of raindrops some of which fragmented. Soon after cloud turrets penetrated above the freezing level, particles from the fragmentation of freezing drops and ice splinter production during riming were probably the main contributors to the production of the extraordinarily high concentrations of ice particles (up to ~1000 litre^{-1} with maximum dimension >100 μm). However, frozen drops and ice fragments were much more numerous than columnar ice crystals <100 μm in maximum dimensions, the latter being indicative of ice splinter production by riming. Some fragmented frozen drops fell out of anvil regions just above the research aircraft, and were intercepted at temperatures lower than −8 °C. Narrow streamers (~10–20 m across) of large (>3 mm diameter) solid and liquid particles were observed in the clouds. These clusters are likely to have originated near cloud tops. Such concentrated shafts of frozen particles falling at appreciable speeds are likely to enhance the produce of splinters by riming lower down in the clouds.

We also found that ice-free clouds, though far narrower overall than clouds containing ice, could produce localized rain rates nearly equal to those from deep clouds containing ice. This suggests that the collision–coalescence of drops and the riming of frozen raindrops were responsible for nearly all of the precipitation in the convective regions of the mesoscale complexes.

Acknowledgements

We thank all those who participated in the KWAJEX field experiments, especially our pilots. This research was supported by NASA grants NAG5-8109 and NAG5-7675 and NSF grants ATM-9901624 and ATM-0314453.

REFERENCES

Ackerman, B. 1959 The variability of the water contents of tropical cumuli. *J. Meteorol.*, **16,** 191–198

1963 Some observations of water contents in hurricanes. *J. Atmos. Sci.*, **20,** 288–298

1967 The nature of the meteorological fluctuations in clouds. *J. Appl. Meteorol.*, **6,** 61–67

Austin, P. H., Baker, M. B., Blyth, A. and Jensen, J. B. 1985 Small-scale variability in warm continental cumulus clouds. *J. Atmos. Sci.*, **42,** 1123–1138

Bader, M., Gloster, J., Brownscombe, J. L. and Goldsmith, P. 1974 The production of sub-micron ice fragments by water droplets freezing in free fall or accretion upon an ice surface. *Q. J. R. Meteorol. Soc.*, **100,** 420–426

Beard, K. V., Johnson, D. B. and Baumgardner, D. 1986 Aircraft observations of large raindrops in warm shallow convective clouds. *Geophys. Res. Lett.*, **13,** 991–994

Bjerknes, J. 1969 Atmospheric teleconnections from the equatorial Pacific. *Mon. Weather Rev.*, **97,** 163–172

Black, R. A. and Hallett, J. 1986 Observations of the distribution of ice in hurricanes. *J. Atmos. Sci.*, **43,** 802–822

Blanchard, D. C. 1951 A verification of the Bally–Dorsey theory of spicule formation on sleet pellets. *J. Meteorol.*, **8,** 268–269

Blyth, A. M., Benestad, R. E. and Krehbiel, P. R. 1997 Observations of supercooled raindrops in New Mexico summertime cumuli. *J. Atmos. Sci.*, **54,** 569–575

Braham R. R. Jr. 1964 What is the role of ice in summer rain showers? *J. Atmos. Sci.*, **21,** 640–645

Brownscombe, J. L. and Hallett, J. 1967 Experimental and field studies of precipitation particles formed by the freezing of supercooled water. *Q. J. R. Meteorol. Soc.*, **93,** 455–473

Byers, H. R. 1952 Example of a flight through a thunderstorm updraft. *Bull. Am. Meteorol. Soc.*, **33,** 211–212

Caylor, I. J. and Illingworth, A. J. 1987 Radar observations of warm rain initiation. *Q. J. R. Meteorol. Soc.*, **113,** 1171–1191

Changnon, S. A 1991 Illinois precipitation research: A focus on cloud and precipitation modification. *Bull. Am. Meteorol. Soc.*, **72,** 567–604

Chisnell, R. F. and Latham, J. 1976 Ice particle multiplication in cumulus clouds. *Q. J. R. Meteorol. Soc.*, **102,** 133–156

Choularton, T. W., Latham, J. and Mason, B. J. 1978 A possible mechanism of ice splinter production during riming. *Nature*, **274,** 791–792

Dye, J. E. and Hobbs, P. V. 1966 The effect of carbon dioxide on the shattering of freezing drops. *Nature*, **209,** 464–466

1968 The influence of environmental parameters on the freezing and fragmentation of suspended water drops. *J. Atmos. Sci.*, **25,** 82–96

Fletcher, N. H. 1962 *The physics of rainclouds*. Cambridge University Press, Cambridge, England

Gamache, J. F. 1990 Microphysical observations in summer MONEX convective and stratiform clouds. *Mon. Weather Rev.*, **118,** 1238–1249

Gunn, R. and Phillips, B. B. 1957 An experimental investigation of the effect of air pollution on the initiation of rain. *J. Meteorol.*, **14,** 272–280

Hallett, J. and Mossop, S. C. 1974 Production of secondary ice particles during the riming process. *Nature*, **249,** 26–28

Hallett, J., Sax, R. I., Lamb, D. and Ramachandra Murty, A. S. 1978 Aircraft measurements of ice in Florida cumuli. *Q. J. R. Meteorol. Soc.*, **104,** 631–651

Harris-Hobbs, R. L. and Cooper, W. A. 1987 Field evidence supporting quantitative predictions of secondary ice production rates. *J. Atmos. Sci.*, **44,** 1071–1082

Herzegh, P. H. and Jameson, A. R. 1992 Observing precipitation through dual-polarization radar measurements. *Bull. Am. Meteorol. Soc.*, **73,** 1365–1374

Heymsfield, A. J. and Parrish, J. L. 1978 A computational technique for increasing the effective sampling volume of the PMS two-dimensional particle size spectrometer. *J. Appl. Meteorol.*, **17,** 1566–1572

Hobbs, P. V. and Alkezweeny, A. J. 1968 The fragmentation of freezing water droplets in free fall. *J. Atmos. Sci.*, **25,** 881–888

Hobbs, P. V. and Rangno, A. L. 1985 Ice particle concentrations in clouds. *J. Atmos. Sci.*, **36,** 2523–2549

1990 Rapid development of ice particle concentrations in small polar maritime cumuliform clouds. *J. Atmos. Sci.*, **47,** 2710–2722.

Hobbs, P. V. and Rangno, A. L. 1998 Microstructures of low and middle-level clouds over the Beaufort Sea. *Q. J. R. Meteorol. Soc.*, **124,** 2035–2071

2004 Super-large raindrops. *Geophys. Res. Lett.*, **31,** L13102, doi:10.1029/2004GL020167

Hou, A. Y. 1998 Hadley circulation as a modulator of the extratropical climate. *J. Atmos. Sci.*, **55,** 2437–2457

Illingworth, A. J. 1988 The formation of rain in convective clouds. *Nature*, **336,** 754–756

Jameson, A. R. and Kostinski, A. B. 1999 Fluctuation properties of precipitation. Part V: Distribution of rain rates—theory and observations in clustered rain. *J. Atmos. Sci.*, **56,** 3920–3932

Jameson, A. R., Murphy, M. J. and Krider, E. P. 1996 Multiple-parameter observations of isolated Florida thunderstorms during the onset of electrification. *J. Appl. Meteorol.*, **35,** 343–354

Johnson, D. B. 1982 The role of giant and ultragiant aerosol particles in warm rain initiation. *J. Atmos. Sci.*, **39,** 448–460

1993 The onset of effective coalescence growth in convective clouds. *Q. J. R. Meteorol. Soc.*, **119,** 925–933

Johnson, D. A. and Hallett, J. 1968 Freezing and shattering of supercooled drops. *Q. J. R. Meteorol. Soc.*, **94,** 468–482

Kaneyasu, N., Hobbs, P. V., Ishizaka, Y. and Qian, G.-W. 2001 Aerosol properties around marine tropical cumulus clouds. *J. Geophys. Res.*, **106,** 14435–14445

Khain, A., Ovtchinnikov, M., Pinsky, M., Pokrovsky, A. and Krugliak, H. 2000 Notes on the state-of-the-art numerical modelling of cloud microphysics. *Atmos. Res.*, **55,** 159–224

Kingsmill, D. K., Yuter, S. E., Heymsfeld, A. J., Hobbs, P. V., Korolev, A. V., Stith, J. L., Bansemer, A., Haggerty, J. A. and Rangno, A. L. 2004 TRMM common microphysics products: A tool for evaluating spaceborne precipitation retrieval algorithms. *J. Appl. Meteorol.*, **43,** 1598–1618

Knight, C. A. and Knight, N. C. 1974 Drop freezing in clouds. *J. Atmos. Sci.*, **31,** 1174–1176

Knight, C. A., Vivekanandan, J. and Lasher-Trapp, S. G. 2002 First radar echoes and the early ZDR history of Florida cumulus. *J. Atmos. Sci.*, **59,** 1454–1472

Koenig, L. R. 1963 The glaciating behavior of small cumulonimbus clouds. *J. Atmos. Sci.*, **20,** 29–47

Kolomeychuk, R. J., McKay, D. C. and Iribarne, J. V. 1975 The fragmentation and electrification of freezing drops. *J. Atmos. Sci.*, **32,** 974–979

Kostinski, A. B. and Jameson, A. R. 1997 Fluctuation properties of precipitation. Part I: On deviations of single-size drop counts from the Poisson distribution. *J. Atmos. Sci.*, **54,** 2174–2186

2000 On the spatial distribution of cloud particles. *J. Atmos. Sci.*, **57,** 901–915

Kunkel, B. A. 1984 Parameterization of droplet terminal velocity and extinction coefficient in fog models. *J. Clim. Appl. Meteorol.*, **23,** 34–41

Lawson, R. P. and Jensen, T. L. 1998 'Improved microphysical observations in mixed phase clouds'. Pp. 451–454 in Preprints: Conference on cloud physics. American Meteorology Society, Boston, USA

Lawson, R. P., Stewart, R. E., Strapp, J. W. and Isaac, G. A. 1993 Airborne measurements of the origin and growth of very large snowflakes. *Geophys. Res. Lett.*, **20,** 53–56

Leary, C. A. and Houze R. A. Jr. 1979 The structure of and evolution of convection in a tropical cloud cluster. *J. Atmos. Sci.*, **36,** 437–457

MacCready, P. B. and Takeuchi, D. M. 1968 Precipitation initiation mechanisms and droplet characteristics of some convective cloud cores. *J. Appl. Meteorol.*, **7,** 591–601

Magono, C., Fujita, S.-I. and Taniguchi, T. 1979 Unusual types of single ice crystals originating from frozen cloud droplets. *J. Atmos. Sci.*, **36,** 2495–2501

Malkus, J. S. 1954 Some results of a trade-cumulus cloud investigation. *J. Meteorol.*, **11,** 220–237

Malkus, J. S. and Ronne, C. 1954 On the structure of some cumulonimbus clouds which penetrated the high tropical troposphere. *Tellus*, **6,** 351–366

Manton, M. J. 1979 On the broadening of a droplet distribution by turbulence near cloud base. *Q. J. R. Meteorol. Soc.*, **105,** 899–914

Mason, B. J. 1971 *The physics of clouds*. Oxford University Press, Oxford, UK

Mason, B. J. and Maybank, J. 1960 The fragmentation and electrification of freezing water drops. *Q. J. R. Meteorol. Soc.*, **86,** 176–186

Mather, G. K., Morrison, B. J. and Morgan, G. M. 1986 A preliminary assessment of the importance of coalescence in convective clouds of the eastern Transvaal. *J. Clim. Appl. Meteorol.*, **25,** 1780–1784

Meyers, M. P., DeMott, P. J. and Cotton, W. R. 1992 New primary ice-nucleation parameterizations in an explicit cloud model. *J. Appl. Meteorol.*, **31,** 708–721

Mordy, W. A. and Eber, L. E. 1954 Observations of rainfall from warm clouds. *Q. J. R. Meteorol. Soc.*, **80,** 48–57

Mosimann, L., Weingartner, E. and Waldvogel, A. 1994 An analysis of accreted drop sizes and mass on rimed snow crystals. *J. Atmos. Sci.*, **51,** 1548–1558

Mossop, S. C. 1985 Secondary ice particle production during rimer growth: The effect of drop size distribution and rimer velocity. *Q. J. R. Meteorol. Soc.*, **111,** 1113–1124

1976 Production of secondary ice particles during the growth of graupel by riming. *Q. J. R. Meteorol. Soc.*, **102,** 45–57

Mossop, S. C. and Ono, A. 1969 Measurements of ice crystal concentrations in clouds. *J. Atmos Sci.*, **26,** 130–137

Mossop, S. C., Ono, A. and Wishart, E. R. 1970 Ice particles in maritime clouds near Tasmania. *Q. J. R. Meteorol. Soc.*, **96,** 487–508

Musil, D. J. and Smith, P. J. 1990 Interior characteristics at mid-levels of thunderstorms in the southeastern United States. *Atmos. Res.*, **24,** 149–167

Ohtake, T., Jayaweera, K. and Sakurai, K.-I. 1982 Observation of ice crystal formation in lower Arctic atmosphere. *J. Atmos. Sci.*, **39,** 2898–2904

Ono, A. 1972 Evidence on the nature of ice crystal multiplication processes in natural cloud. *J. Res. Atmos.*, **6,** 399–408

Petty, G. W. 1999 Prevalence of precipitation from warm-topped clouds over eastern Asia and the western Pacific. *J. Climate*, **12,** 220–229

Phillips, V. T. J., Blyth, A. M., Brown, P. R. A., Choularton, T. W. and Latham, J. 2001 The glaciation of a cumulus cloud over New Mexico. *Q. J. R. Meteorol. Soc.*, **127,** 1513–1534

Pinsky, M. and Khain, A. P. 1997 Formation of inhomogeneity in drop concentration induced by drop inertia and their contribution to the drop spectrum broadening. *Q. J. R. Meteorol. Soc.*, **123,** 165–186

2001 Fine structure of cloud droplet concentrations as seen from the fast-FSSP measurements. Part I: Method of analysis and preliminary results. *J. Appl. Meteorol.*, **40,** 1515–1537

2002 Effects of in-cloud nucleation and turbulence on droplet spectrum formation in cumulus clouds. *Q. J. R. Meteorol. Soc.*, **128,** 501–533

Pitter, R. L. and Pruppacher, H. R. 1973 A wind tunnel investigation of freezing of small water drops falling at terminal velocity in air. *Q. J. R. Meteorol. Soc.*, **99,** 540–550

Plank, V. G., Atlas, D. and Paulsen, W. H. 1955 The nature and detectability of clouds and precipitation as determined by 1.25 cm radar. *J. Meteorol.*, **12,** 358–378

Pruppacher, H. R. and Klett, J. D. 1997 *The microphysics of clouds and precipitation.* Kluwer Academic Press, Dordrecht, the Netherlands

Pruppacher, H. R. and Schlamp, R. J. 1975 A wind tunnel investigation on ice multiplication by freezing of water drops falling at terminal velocity in air. *J. Geophys. Res.*, **80,** 380–385

Rangno, A. L. 1988 Rain from clouds with tops warmer than −10 °C in Israel. *Q. J. R. Meteorol. Soc.*, **114,** 495–513

Rangno, A. L. and Hobbs, P. V. 1983 Production of ice particles in clouds due to aircraft penetrations. *J. Clim. Appl. Meteorol.*, **22,** 214–237

1991 Ice particle concentrations and precipitation development in small polar maritime cumuliform clouds. *Q. J. R. Meteorol. Soc.*, **117,** 207–241

1994 Ice particle concentrations and precipitation development in small continental cumuliform clouds. *Q. J. R. Meteorol. Soc.*, **120,** 573–601

2001 Ice particles in stratiform clouds in the Arctic and possible mechanisms for the production of high ice concentrations. *J. Geophys. Res.*, **106,** 15064–15075

Rasmussen, R. M., Bernstein, B. C., Murakami, M., Stossmeister, G. and Reisner, J. 1995 The 1990 Valentine's Day arctic outbreak. Part I: Mesoscale and microscale structure and evolution of a Colorado Front Range shallow upslope cloud. *J. Appl. Meteorol.*, **34,** 1481–1511

Rauber, R. M., Beard, K. V. and Andrews, B. A. 1991 A mechanism for giant raindrop formation in warm shallow convective clouds. *J. Atmos. Sci.*, **48,** 1791–1797

Rosenfeld, D. 2000 Suppression of rain and snow by urban and industrial air pollution. *Science*, **287,** 1793–1796

Rosenfeld, D. and Gutman, G. 1994 Retrieving microphysical properties near the tops of potential rain clouds by multispectral analysis of AVHRR data. *J. Atmos. Sci.*, **34,** 259–283

Rosenfeld, D. and Lensky, I. M. 1998 Satellite-based insights into precipitation formation processes in continental and maritime convective clouds. *Bull. Am. Meteorol. Soc.*, **79,** 2457–2476

Saunders, P. M. 1965 Some characteristics of tropical marine showers. *J. Atmos. Sci.*, **22,** 167–173

Sato, N. and Kikuchi, K. 1989 *In situ* growth experiments of snow crystals of low temperature types observed at Inuvik in Arctic Canada. *J. Fac. Sci.*, Hokkaido University, **8,** 333–354

Scott, B. C. and Hobbs, P. V. 1977 A theoretical study of the mixed-phase cumulus clouds. *J. Atmos. Sci.*, **34,** 812–826

Shaw, R. A., Reade, W. C., Collins, L. R. and Verlinde, J. 1998 Preferential concentration of cloud droplets by turbulence: Effects on the early evolution of cumulus cloud droplet spectra. *J. Atmos. Sci.*, **55,** 1965–1976

Simpson, J., Adler, R. F. and North, G. R. 1986 On the Tropical Rainfall Measuring Mission (TRMM). *Meteorol. Atmos. Phys.*, **60,** 19–36

1988 A proposed Tropical Rainfall Measuring Mission (TRMM) satellite. *Bull. Am. Meteorol. Soc.*, **69,** 278–295

Smith, M. H., Park, P. M. and Consterdine, I. E. 1993 Marine aerosol concentrations and estimated fluxes over the sea. *Q. J. R. Meteorol. Soc.*, **119,** 809–824

SPEC 2000 'SPEC cloud particle imager: Operator's manual'. Stratton Park Engineering Company Inc., 5401 Western Avenue, Boulder, Colorado 80301, USA

Squires, P. 1958a The microstructure and colloidal stability of warm clouds. Part I. The relation between structure and stability. *Tellus*, **10,** 256–261

1958b The microstructure and colloidal stability of warm clouds. Part II. The causes of variations in microstructure. *Tellus*, **10,** 262–271

1958c The spatial variation of liquid water and droplet concentration in cumuli. *Tellus*, **10,** 372–380

Stith, J. L., Dye, J. E., Bansemer, A., Heymsfield, A. J., Grainger, C. A., Petersen, W. A. and Cifelli, R. 2002 Microphysical observations of tropical clouds. *J. Appl. Meteorol.*, **41,** 97–117

Stith, J. L., Haggerty, J. A., Heymsfield, A. and Grainger, C. A. 2004 Microphysical characteristics of tropical updrafts in clean conditions. *J. Appl. Meteorol.*, **43,** 779–794

Szumowski, M. J., Rauber, R. M., Ochs III, H. T. and Miller, L. J. 1997 The microphysical structure and evolution of Hawaiian rainband clouds. Part I: Radar observations of rainbands containing high reflectivity cores. *J. Atmos. Sci.*, **54,** 369–385

Takaya, Y. 1993 The motion of uneven structure of convective clouds. *J. Atmos. Sci.*, **50,** 574–587

Twomey, S. 1959 The nuclei of natural cloud formation. Part II: The supersaturation in natural clouds and the variation of cloud droplet concentration. *Geofis. Pura Appl.*, **43,** 243–249

Wallace, J. M. and Hobbs, P. V. 1977 *Atmospheric science: An introductory survey.* Academic Press, New York, USA

Willis, P. T., Hallett, J., Black, R. A. and Hendricks, W. 1994 An aircraft study of rapid precipitation development and electrification in a growing convective cloud. *Atmos. Res.*, **33,** 1–24

Yuter, S. E. and Houze, R. A. Jr. 1998 The natural variability of precipitating clouds over the western Pacific warm pool. *Q. J. R. Meteorol. Soc.*, **124,** 53–99

Yuter, S. E., Houze, R. A. Jr., Smith, E. A., Wilheit, T. T. and Zipser, E. 2005 Physical characterization of tropical oceanic convection observed in KWAJEX. *J. Appl. Meteorol.*, in press

Zeng, Z., Yuter, S. E. and Houze R. A. Jr. 2001 Microphysics of the rapid development of heavy convective precipitation. *Mon. Weather Rev.*, **129,** 1882–1904